Energy, Mines and Resources Canada | Énergie, Mines et Ressources Canada

CANMET

Canada Centre for Mineral and Energy Technology | Centre canadien de la technologie des minéraux et de l'énergie

Mining Research Laboratories | **Laboratoires de recherche minière**

Canada

MRL 88-104(TR) c.2

UNIAXIAL MECHANICAL AND DYNAMIC PROPERTIES OF ANOMOLOUS ROCK SAMPLES FROM LAC DU BONNET, MANITOBA: REPORT #2

R. Jackson

MRL 88-104(TR)

UNIAXIAL MECHANICAL AND DYNAMIC PROPERTIES OF ANOMOLOUS ROCK SAMPLES FROM LAC DU BONNET, MANITOBA

by

Rand Jackson*

ABSTRACT

Compressive and shear wave velocity measurements, as well as uniaxial compression testing, were conducted on samples of dike and xenolith material exposed during shaft sinking at Atomic Energy of Canada Ltd.'s underground research laboratory (URL). Four rock types were included for testing, these being; granodiorite, heterogeneous coarse to pegmatitic leucocratic granite, amphibolite and homogeneous leucocratic granite.

The purpose of the study is to determine the mechanical properties of the inclusions in the Lac du Bonnet batholith in the vicinity of the URL. The resulting data is compared to an earlier test series conducted on the same rock types.

---

*Research Officer, Canadian Mine Technology Laboratories, CANMET, Energy, Mines and Resources Canada, Ottawa, Ontario.

Keywords

Rock Properties, Mechanical, Young's Modulus, Poisson's Ratio, Uniaxial Compressive Strength, Velocity, Lac du Bonnet

PROPRIÉTÉS MÉCANIQUES ET DYNAMIQUES UNIAXIALES DES ÉCHANTILLONS DE ROCHE IRRÉGULIERS EN PROVENANCE DU LAC DU BONNET (MANITOBA)

par

Rand Jackson*

RÉSUMÉ

On a mésure la vitesse des ondes de compression et de cisaillement (onde transversale) et mené des essais de compression uniaxiale sur des échantillons de xénolithe et de roche filonienne. Ces échantillons ont été mis à découvert lors du foncage de puits au Laboratoire de recherche souterrain (LRS) de L'Énergie Atomique du Canada Limitée. Quatre types de roches ont été soumises aux essais, soit la granodiorite, le granite leucarate hétérogène à gros grains ou à structure pegmatique, l'amphibolite et le granite leucocrate homogène.

L'étude vise à déterminer les propriétés mécaniques des inclusions dans le batholithe du Lac du Bonnet qui gît à proximité du Laboratoire de recherche souterrain. On compare les données obtenues aux résultats de la série d'essais antérieurs qui ont été menés sur des roches de même type.

---

*Chercher scientifique, Laboratoire canadien de technologie minière, CANMET, Énergie, Mines et Ressources Canada, Ottawa (Ontario).

Mots clés

Propriétés des roches; mécanique; module de Young; rapport de Poisson; résistance à la compression uniaxiale, vitesse, Lac du Bonnet.

CONTENTS

TABLES

FIGURES

INTRODUCTION

As part of the Canadian Nuclear Fuel Waste Management Project, Atomic Energy of Canada Limited is characterizing various rock formations within the Canadian Shield to determine their suitability for the long term disposal of high level wastes. The program also includes the construction of an underground research laboratory (URL) near Pinawa, Manitoba to provide an opportunity for extensive in situ investigations.

During shaft sinking at the URL site, several anomalous rock types were uncovered in the form of dikes and xenoliths. Determining the mechanical properties of these formations is necessary in order to better model the response of the rock mass to expected changes in the in situ stress field caused by excavation and testing. The five major rock types chosen for testing include; amphibolite, heterogeneous coarse to pegmatitic leucocratic granite, homogeneous leucocratic granite, pegmatite and granodiorite. These have been designated as rock types 4, 5B, 5C, 6 and 7, respectively by investigators at the site (Read, 1987).

A previous study (Jackson, 1988), summarizes unconfined velocity and uniaxial compression test results for the five rock types just mentioned. The purpose of the program described here is to provide support data for the earlier study and to identify those rock types which may require additional characterization. Rock type 6 is not, however, represented due to insufficient core availability.

IDENTIFICATION OF SPECIMENS AND TESTS

Thirty-seven samples originating from boreholes 201-011-HG2, 209-025-SV2, 209-021-SV1 and 209-018-EXT4 were prepared for uniaxial compression testing. Of these, 10 of rock type 4, 8 of rock type 5B, 12 of rock type 5C and 7 of rock type 7 were tested. Table 1 provides a summary of the specimen depth, dimensions and density. The following properties were determined for the samples listed;

1) compressive wave velocity
2) shear wave velocity
3) dynamic shear modulus, G_d
4) dynamic Young's modulus, E_d
5) Poisson's ratio (determined using velocity data)
6) uniaxial compressive strength
7) Poisson's ratio
8) tangent moduli of elasticity, E_t

Table 1: Summary of Specimen Dimensions and Density

Rock type	Drill hole	Sample depth (m)	Length (mm)	Diameter (mm)	Density (gm/cc)
4	201-011-HG2	112.17	130.16	60.90	2.71
		112.30	131.17	60.88	2.72
		112.44	129.572	60.89	2.71
		112.58	128.28	60.88	2.69
		137.20	132.69	61.00	2.71
		137.33	128.37	61.00	2.86
		137.47	127.86	61.00	2.81
		137.72	128.35	61.00	2.72
		137.85	130.00	61.00	2.70
		137.99	127.81	61.00	2.68
5B	209-025-SV2	1.76	96.64	45.05	2.65
		1.87	97.03	45.04	2.65
		1.97	94.94	44.90	2.64
		2.24	96.09	44.98	2.64
		2.56	95.36	45.03	2.63
		2.66	94.82	45.02	2.63
		11.91	98.64	44.97	2.61
		12.01	93.75	44.97	2.63
5C	209-021-SV1	11.55	94.28	45.00	2.64
		11.67	98.74	45.00	2.60
		11.86	97.89	45.01	2.61
		11.97	97.20	44.99	2.61
		12.14	94.43	45.00	2.61
		12.25	98.10	45.00	2.61
		12.39	97.15	45.01	2.61
		12.50	99.91	45.01	2.61
		12.65	97.00	45.02	2.62
		12.77	98.67	45.03	2.60
		12.88	97.49	44.99	2.61
		12.98	95.54	45.00	2.62

Table 1: cont'd

Rock type	Drill hole	Sample depth (m)	Length (mm)	Diameter (mm)	Density (gm/cc)
7	209-018-EXT4	13.98	98.03	44.99	2.67
		14.14	95.60	44.98	2.68
		14.25	96.41	44.99	2.67
		14.35	96.79	44.99	2.68
		14.46	98.60	44.99	2.67
		14.56	97.99	44.99	2.67
		15.18	98.13	44.99	2.67

DESCRIPTION OF TEST MEASUREMENTS

Compression and shear wave velocity measurements were carried out on samples prior to being gauged for elastic deformation measurement. The testing equipment consisted of: transmitting and receiving platens containing piezoelectric transducers, a high voltage pulse generator, a signal amplifier and a Tektronix Type 555 dual beam oscilloscope equipped with delay sweep and a time base resolution of 0.01 micro-seconds.

For an outline of the uniaxial compression procedure, the reader is referred to Technical Data 303410-M01/78 (2). The two Phillips PR 9302 strain bridges and the Mosely Autograph 2FRA X-Y recorder referred to in that document were replaced, in the present study, by two Bruel and Kjaer Type 1526 strain indicators and a Hewlett Packard 7046B X-Y recorder. These equipment were used to measure and record the axial and transverse strains as a function of axial load. Linear variable differential transducers (LVDT's) were also utilized to provide redundant measurements of axial deformation.

Load was applied at a rate of 1 kN/sec until 50 MPa after which actuator control was governed by circumferential strain. This enabled the operator to control the violent, brittle failure usually associated with high strength rock and avoid damage to the lvdt's. This method, however, resulted in very low loading rates being applied just prior to and at failure, the results of which will be discussed later.

DATA TREATMENT

The compressional and shear wave velocities were determined by dividing the specimen length by the wave travel time through the specimen. The dynamic properties were then calculated using the following equations (3);

Dynamic Young's Modulus

$$E_d = \frac{\rho V_s^2 (3V_p^2 - 4V_s^2)}{V_p^2 - V_s^2} \tag{1}$$

where; E_d =dynamic Young's modulus
V_s =shear wave velocity
V_p =compressional wave velocity
ρ =density

Dynamic Shear Modulus

$$G_d = \rho V_s^2 \tag{2}$$

where; G_d =dynamic shear modulus
V_s =shear wave velocity
ρ =density

Poisson's Ratio (based on velocity data)

$$\nu_d = \frac{V_p^2 - 2V_s^2}{2(V_p^2 - V_s^2)} \tag{3}$$

where; ν_d =Poisson's ratio
V_s =shear wave velocity
V_p =compressional wave velocity

Stress-strain curves were computer generated using analog outputs from the strain bridges and press. Tangent moduli of elasticity were calculated for each sample at stress levels of 10, 20, 30, 40, 50 and 60 MPa and 10%, 20%, 30%, 40%, 50%, and 75% of ultimate strength. The ultimate compressive strength of each sample was calculated by dividing the failure load by the sample's cross-sectional area. The ratio of the tangent to the axial strain curve to the tangent to the transverse strain curve at 50% failure load was used to determine the sample's Poisson's ratio (ν).

DATA SUMMARY

Tables 2 to 5 contain ultrasonic velocity measurements for rock types 4, 5B, 5C and 7 respectively. These include the calculated values of the compressive and shear wave velocities dynamic shear modulus, dynamic Young's modulus as well as Poisson's ratio estimated on the basis of velocity results for each sample. Ultrasonic velocity data was not available for specimen numbers 1.76, 1.87, 1.97 and 11.91 of borehole 209-025-SV2.

Tables 6 to 9 summarize uniaxial compression data which include uniaxial compressive strength, tangent moduli of elasticity and Poisson's ratio for rock types 4, 5B, 5C and 7, respectively.

Table 10 presents the dynamic and uniaxial compressive property means and standard deviations of the four rock types used for this study. Table 11 presents the same data for specimens used in the previous study of these rock types.

Figures 1 through 37 represent the circumferential and axial stress/strain curves for each sample. Figure 38 illustrates the difference between testing in load as opposed to circumferential strain control.

OBSERVATIONS

In comparing the mean results of this and the previous test program, several significant differences can be seen (see Tables 10 and 11). The most profound of these is the consistently lower uniaxial compressive strengths determined for the second series.

As mentioned earlier, circumferential strain was chosen as the control mode in the present study to avoid damage to the lvdt's. Unfortunately, as the specimen nears failure, circumferential strain begins to increase dramatically and the loading rate must decrease accordingly to maintain a constant strain rate. Figure 38 illustrates a typical load vs. time curve resulting from a circumferential control signal as opposed to a fixed loading rate.

Several investigators have studied the effect of loading rate on uniaxial compressive strength (Houpert, 1970, Perkins, Green and Friedman, 1970), and, in general, it has been shown that strength will decrease as the loading rate decreases. The lower loading rates of the current program, therefore, have resulted in decreases of 18%, 17% and 12% in compressive strength for rock types 5B, 5C and 7, respectively.

Rock type 4 exhibited the largest difference in strength, dropping from a mean value of 231 MPa in the first test series to 140 in the second. It's unlikely, however, that slower loading rates could affect this degree of change. Rather, significant structural differences exist between the two sample suites to account for the observed behaviour. This is clearly indicated by differences in their respective densities and 50% tangent moduli. A mean density of 2.98 g/cc ($\sigma^2 = 0.03$) and mean 50% tangent modulus of 87.47 GPa ($\sigma^2 = 8.04$) were determined for the original sample set while corresponding values of 2.73 g/cc ($\sigma^2 = 0.06$) and 67.53 GPa ($\sigma^2 = 3.00$) were exhibited by the second. While no petrographic analysis has been done, visual inspection of the suites also indicated that the original program's samples showed considerably more compositional variation than those of the second set.

With the exception of rock type 4, the 50% tangent moduli of the second set of results were somewhat lower than those determined for the first set. Rock type 5B, in particular, showed a considerable increase in modulus of 22% from one test series to the next. These differences, however, are likely explained by the usual statistical variation inherent in rock testing.

In terms of dynamic properties, the second sample set exhibited slightly higher compressive wave velocities than those observed for the first set. Shear wave velocities, however, showed little variation from one study to the next with the exception of rock type 4 whose S-wave velocity decreased from 3.61 km/sec to 2.82 km/sec (22%). The resulting dynamic shear and Young's moduli were much more consistent from rock type to rock type for the second set of samples than for the first (see Tables 10 and 11). It is also interesting to note that, for whatever reason, the dynamic Young's moduli determined as part of this study correspond best with a static tangent moduli associated with axial loads of between 10 and 20 MPa as opposed to 0.10 MPa which might be anticipated.

RECOMMENDATIONS

The long term nature of a nuclear waste disposal site and the stress concentrations resulting from its possible construction deep in igneous rock makes an understanding of the effect of various rates of loading on compressive strength important. This study indicates that, at least for the rock types tested, strength differences on the order of 10 to 20% can occur with a change in loading rate even while staying within ASTM standards. It is recommended, then, that a program be conducted to study what the effect of loading rates on the order of hours and possibly days will be on the gray granite encountered at the URL site.

The mean mechanical properties of rock type 4 vary considerably from the first test program to the second. While this may be due, in part, to differences in testing technique, there appears to be considerable structural variation from one sample suite to the next. Some distinction should be made between the two suites by carrying out either petrographic analyses on representative samples or additional mechanical testing or both.

Rock types 5C and 7 results are not dissimilar enough to warrant additional characterization with any differences in mechanical properties being attributable to changes in the testing technique. The 22% variation in modulus of rock type 5B from one test series to the next, however, may be sufficient to warrant additional study. Testing of another sample suite of rock type 6 is adviseable should additional core become available.

Circumferential strain will no longer be used as a control mode for uniaxial compression measurements and loading rates of between 0.5 and 1.0 MPa will be adhered to in any future test programs related to AECL work.

Table 2 - Summary of Ultrasonic Velocity Properties: Rock Type 4

Drill Hole	Sample Depth (m)	P-wave Velocty (km/sec)	S-wave Velocity (km/sec)	Dynamic Shear Modulus (GPa)	Dynamic Young's Modulus (GPa)	Poisson's Ratio
201-011-HG2	112.17	5.11	2.73	20.20	52.51	0.10
	112.30	5.04	2.75	20.54	52.95	0.09
	112.44	4.96	2.73	20.24	51.92	0.08
	112.58	5.31	2.82	21.49	55.99	0.12
	137.20	5.06	2.85	22.01	55.81	0.08
	137.33	5.40	2.94	24.87	64.19	0.12
	137.47	5.28	2.87	23.19	59.82	0.11
	137.72	5.28	2.88	22.52	58.06	0.11
	137.85	5.02	2.84	21.84	55.20	0.08
	137.99	5.29	2.83	21.41	55.68	0.12

Table 3 - Summary of Ultrasonic Velocity Properties: Rock Type 5B

Drill Hole	Sample Depth (m)	P-wave Velocty (km/sec)	S-wave Velocity (km/sec)	Dynamic Shear Modulus (GPa)	Dynamic Young's Modulus (GPa)	Poisson's Ratio
209-025-SV2	2.24	5.32	2.79	20.51	53.74	0.13
	2.56	5.29	2.70	19.26	50.96	0.14
	2.66	5.20	2.70	19.25	50.62	0.12
	12.01	5.11	2.58	17.43	46.38	0.13

Table 4 - Summary of Ultrasonic Velocity Properties: Rock Type 5C

Drill Hole	Sample Depth (m)	P-wave Velocty (km/sec)	S-wave Velocity (km/sec)	Dynamic Shear Modulus (GPa)	Dynamic Young's Modulus (GPa)	Poisson's Ratio
209-021-SV1	11.55	5.39	2.72	19.59	52.08	0.15
	11.67	4.99	2.76	19.89	50.87	0.08
	11.86	5.27	2.85	22.47	57.18	0.10
	11.97	5.19	2.86	21.21	54.83	0.11
	12.14	5.00	2.61	21.32	54.69	0.10
	12.25	5.08	2.75	19.79	51.11	0.10
	12.39	5.23	2.79	20.33	52.91	0.11
	12.50	5.01	2.73	19.40	50.03	0.09
	12.65	5.23	2.72	19.36	50.94	0.13
	12.77	5.10	2.67	18.52	48.58	0.11
	12.88	5.07	2.72	19.23	49.96	0.10
	12.98	5.02	2.62	18.00	47.25	0.11

Table 5 - Summary of Ultrasonic Velocity Properties: Rock Type 7

Drill Hole	Sample Depth (m)	P-wave Velocty (km/sec)	S-wave Velocity (km/sec)	Dynamic Shear Modulus (GPa)	Dynamic Young's Modulus (GPa)	Poisson's Ratio
209-018-EXT4	13.98	5.23	2.80	21.02	54.59	0.11
	14.14	5.27	2.83	21.47	55.70	0.12
	14.25	5.27	2.84	21.55	55.86	0.12
	14.35	5.34	2.97	23.68	60.40	0.11
	14.46	5.35	3.00	24.08	61.18	0.10
	14.56	5.39	2.98	23.77	60.82	0.11
	15.18	5.31	2.94	23.12	59.12	0.11

Table 6: Summary of Uniaxial Compression Properties: Rock Type 4

Specimen Identification	Uniaxial Compressive Strength (MPa)	Tangent Modulus of Elasticity (GPa)												Poisson's Ratio
		10 MPa	20 MPa	30 MPa	40 MPa	50 MPa	60 MPa	10%	20%	30%	40%	50%	75%	
201-011-HG2 112.17	139	45.80	53.34	58.06	61.26	63.24	64.15	49.29	57.15	61.66	63.87	64.56	57.17	0.34
112.30	136	51.47	59.06	62.46	64.80	66.24	66.85	55.23	61.57	64.91	66.58	67.08	61.37	0.26
112.44	136	53.64	62.57	66.54	69.27	70.91	71.59	58.12	65.56	69.43	71.32	71.88	65.01	0.31
112.58	140	53.03	60.91	64.29	66.51	67.72	67.99	57.41	63.72	66.84	68.00	67.84	59.01	0.31
137.20	144	51.90	58.29	61.84	64.28	65.76	66.36	55.43	61.50	64.87	66.29	66.03	59.32	0.31
137.33	114	51.18	57.63	61.15	63.08	63.60	62.76	52.37	58.77	62.12	63.53	63.18	53.56	0.30
137.47	149	51.98	59.19	63.32	66.23	68.12	69.10	56.27	63.26	67.25	69.08	69.04	62.39	0.37
137.72	140	53.35	59.76	62.81	64.83	65.95	66.21	56.78	62.29	65.13	66.21	65.86	58.33	0.25
137.85	142	48.93	57.00	61.26	64.22	66.11	67.04	53.29	60.68	64.82	66.85	67.16	61.92	0.30
137.99	159	56.97	64.76	68.18	70.63	72.25	73.09	62.73	68.67	71.94	73.22	72.66	66.14	0.28

Table 7: Summary of Uniaxial Compression Properties: Rock Type 5B

Specimen Identification	Uniaxial Compressive Strength (MPa)	Tangent Modulus of Elasticity (GPa)												Poisson's Ratio
		10 MPa	20 MPa	30 MPa	40 MPa	50 MPa	60 MPa	10%	20%	30%	40%	50%	75%	
209-025-SV2 1.76	183	46.77	55.25	61.74	66.48	69.93	72.30	53.90	65.01	71.19	74.05	74.69	67.16	0.22
1.87	175	41.29	50.87	58.10	63.06	66.39	68.37	48.39	60.64	66.88	69.12	69.98	69.64	
1.97	131	53.05	60.43	64.85	68.24	70.79	72.61	56.32	63.29	68.02	71.28	73.26	69.83	0.13
2.24	156	54.96	63.67	69.31	73.00	75.11	75.81	60.36	69.81	74.57	75.78	74.85	76.63	0.19
2.56	168	50.94	59.07	64.73	68.46	70.65	71.48	56.50	66.03	70.58	71.36	70.46	69.72	0.36
2.66	100	51.48	58.51	62.72	65.47	67.00	67.42	51.49	58.52	62.73	65.48	67.01	66.54	
11.91	139	40.56	52.31	60.09	64.89	67.52	68.28	45.40	58.70	65.49	68.17	67.54	77.29	0.24
12.01	166	47.24	57.94	65.24	69.83	72.36	73.10	54.50	66.86	72.27	72.73	71.65	76.50	0.27

Table 8: Summary of Uniaxial Compression Properties: Rock Type 5C

Specimen Identification	Uniaxial Compressive Strength (MPa)	Tangent Modulus of Elasticity (GPa)												Poisson's Ratio
		10 MPa	20 MPa	30 MPa	40 MPa	50 MPa	60 MPa	10%	20%	30%	40%	50%	75%	
209-021-SV1 11.55	155	52.42	64.37	72.72	78.32	81.87	83.69	59.36	73.43	80.86	83.88	83.48	89.47	0.50
11.67	178	44.39	54.28	61.14	65.73	68.59	70.01	51.99	63.58	69.02	70.14	69.15	68.22	0.33
11.86	196	50.18	57.75	62.36	65.63	67.80	69.00	57.56	65.44	68.92	69.37	68.79	63.29	0.27
11.97	199	46.26	54.29	59.61	63.34	65.84	67.27	54.21	63.26	67.23	67.88	67.40	61.57	0.23
12.14	173	37.69	49.98	58.57	64.47	68.52	71.11	46.97	61.55	69.11	72.41	73.44	69.48	0.27
12.25	182	41.12	50.99	57.79	62.48	65.64	67.54	49.44	60.96	66.64	68.34	67.96	62.06	0.25
12.39	192	50.35	58.32	63.76	67.46	69.78	70.89	57.71	66.89	70.70	70.80	70.10	66.60	0.35
12.50	165	45.49	55.16	61.61	66.04	68.96	70.59	51.90	62.72	68.55	70.94	71.09	69.46	0.31
12.65	172	48.09	58.48	65.53	70.25	73.22	74.70	55.96	67.86	73.56	74.86	74.08	69.89	0.22
12.77	153	46.22	55.12	61.10	65.18	67.81	69.19	51.41	61.37	66.88	69.27	69.38	66.46	0.33
12.88	187	47.75	55.46	60.83	64.49	66.80	67.94	54.59	63.66	67.62	68.00	67.60	65.38	0.27
12.98	180	43.32	52.84	59.26	63.65	66.50	68.07	51.22	62.08	67.26	68.55	68.31	63.82	0.27

Table 9: Summary of Uniaxial Compression Properties: Rock Type 7

Specimen Identification	Uniaxial Compressive Strength (MPa)	Tangent Modulus of Elasticity (GPa)												Poisson's Ratio
		10 MPa	20 MPa	30 MPa	40 MPa	50 MPa	60 MPa	10%	20%	30%	40%	50%	75%	
209-018-EXT4 13.98	223	42.42	51.34	58.30	63.02	66.08	67.76	53.15	64.57	68.26	68.99	68.66	62.88	0.27
14.14	226	47.79	56.21	62.18	65.96	68.03	68.56	58.04	67.25	69.19	69.58	68.95	62.36	0.29
14.25	229	48.70	56.04	61.17	64.83	67.31	68.78	57.69	66.38	69.30	69.33	68.50	62.26	0.32
14.35	227	49.71	57.19	62.24	65.81	68.20	69.57	58.71	67.23	66.99	69.78	68.62	60.84	0.33
14.46	231	51.13	57.98	62.65	66.03	68.34	69.72	59.59	67.58	70.29	69.76	68.57	62.27	0.37
14.56	229	49.42	56.81	62.17	65.86	68.24	69.46	58.57	67.39	69.68	69.24	68.12	61.99	0.36
15.18	234	49.24	57.45	63.55	67.77	70.53	72.05	59.69	69.72	72.46	72.28	71.22	64.19	0.33

Table 10: Mean Ultra-sonic and Uniaxial Mechanical Properties: Second Test Series

Mechanical Property	Stress Level	Rock Type 4	5B	5C	7
Compressive Strength (MPa)		140 (11)	152 (27)	178 (15)	228 (4)
Poisson's Ratio	50%	0.30 (0.04)	0.24 (0.08)	0.30 (0.07)	0.32 (0.04)
Tangent Modulus of Elasticity (GPa)	10 MPa	51.82 (2.96)	48.29 (5.29)	46.11 (4.13)	48.34 (2.80)
	20 MPa	59.25 (3.13)	57.26 (4.24)	55.59 (3.83)	56.15 (2.22)
	30 MPa	62.99 (2.86)	63.35 (3.47)	62.02 (4.00)	61.75 (1.68)
	40 MPa	65.51 (2.79)	67.43 (3.13)	66.42 (4.27)	65.61 (1.44)
	50 MPa	66.99 (2.97)	69.97 (2.95)	69.28 (4.46)	68.10 (1.34)
	60 MPa	67.51 (3.13)	71.17 (2.90)	70.83 (4.54)	69.41 (1.35)
	10%	55.69 (3.62)	53.36 (4.79)	53.53 (3.69)	57.92 (2.23)
	20%	62.32 (3.28)	63.61 (4.07)	64.40 (3.58)	67.16 (1.53)
	30%	65.90 (3.12)	68.97 (3.89)	69.69 (4.01)	69.45 (1.70)
	40%	67.49 (3.04)	71.00 (3.32)	71.20 (4.48)	69.85 (1.11)
	50%	67.53 (3.00)	71.18 (3.00)	70.90 (4.51)	68.95 (1.03)
	75%	60.42 (3.74)	71.66 (4.43)	67.98 (7.36)	62.40 (1.01)
P-wave Velocity (km/sec)	0.10 MPa	5.18 (0.15)	5.23 (0.09)	5.13 (0.13)	5.31 (0.06)
S-wave Velocity (km/sec)	0.10 MPa	2.82 (0.07)	2.69 (0.09)	2.73 (0.08)	2.91 (0.08)
Dynamic Shear Modulus (GPa)	0.10 MPa	21.83 (1.44)	19.11 (1.27)	19.93 (1.25)	22.67 (1.28)
Dynamic Young's Modulus (GPa)	0.10 MPa	56.21 (3.72)	50.42 (3.04)	51.70 (2.82)	58.24 (2.77)
Dynamic Poisson's Ratio	0.10 MPa	0.10 (0.02)	0.13 (0.01)	0.11 (0.02)	0.11 (0.01)

*Note: Values in brackets represent one standard deviation.

Table 11: Mean Ultra-sonic and Uniaxial Mechanical Properties: First Test Series

Mechanical Property	Stress Level	Rock Type 4	5B	5C	7
Compressive Strength (MPa)		231 (46)	185 (31)	214 (18)	258 (46)
Poisson's Ratio	50%	0.28 (0.03)	0.25 (0.05)	0.24 (0.03)	0.28 (0.02)
Tangent Modulus (GPa)	50%	87.47 (8.04)	58.58 (9.53)	66.64 (5.41)	64.46 (4.62)
P-wave Velocity (km/sec)	0.10 MPa	5.10 (0.17)	4.32 (0.31)	4.41 (0.23)	4.52 (0.17)
S-wave Velocity (km/sec)	0.10 MPa	3.61 (0.17)	2.87 (0.27)	2.78 (0.12)	2.93 (0.06)
Dynamic Shear Modulus (GPa)	0.10 MPa	40.00 (3.94)	21.47 (4.22)	20.11 (1.68)	22.83 (0.97)
Dynamic Young's Modulus (GPa)	0.10 MPa	74.07 (14.13)	44.74 (4.46)	46.82 (3.44)	52.02 (2.79)
Dynamic Poisson's Ratio	0.10 MPa	-0.01 (0.06)	0.07 (0.20)	0.17 (0.05)	0.14 (0.03)

*Note: Values in brackets represent one standard deviation.

REFERENCES

1. Annor, A. and Geller, L., "Dilatational velocity, Young's modulus, Poisson's ratio, uniaxial compressive strength and Brazilian tensile strength for WN1 and WN2 samples", CANMET/MRL Technical Data 303410-M01/78, 1978.

2. Houpert, R., "The uniaxial compressive strength of rocks", Proc. 2nd Cong. Int. Soc. Rock Mech., Belgrade, Vol. 2, pp. 49-55, 1970.

3. Jackson, R., "Uniaxial mechanical and dynamic properties of anomolous rock samples from Lac du Bonnet Manitoba", CANMET Division Report MRL 87-158(TR), 1987.

4. Jaeger, C., "Rock mechanics and engineering", Cambridge University Press, London, 1972.

5. Perkins, R.D., Green, S.J. and Friedman, M., "Uniaxial stress behaviour of porphyritic tonalite at strain rates to 10^3/second", Int. J. Rock Mech. Min. Sci., Vol. 7, No. 5, pp. 527-535, Sept., 1970.

6. Read, R., "Personal communication", 1987.

7. Touloukian, Y.S. and Ho, C.Y., "Physical properties of rocks and minerals", Volume II-2, McGraw-Hill Book Co., 1981.

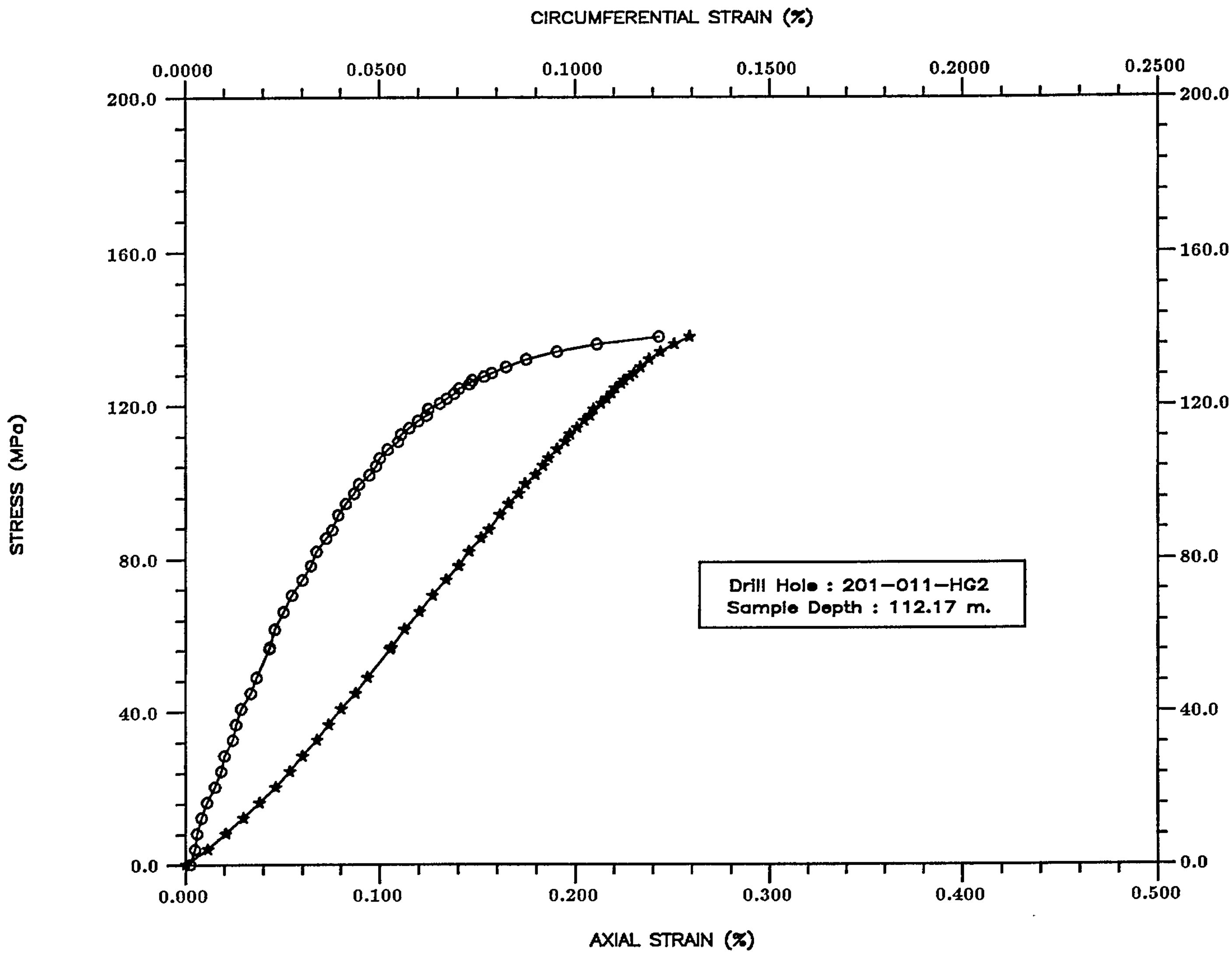

Fig. 1: Axial and circumferential stress/strain curves for anomolous uniaxial test specimens.

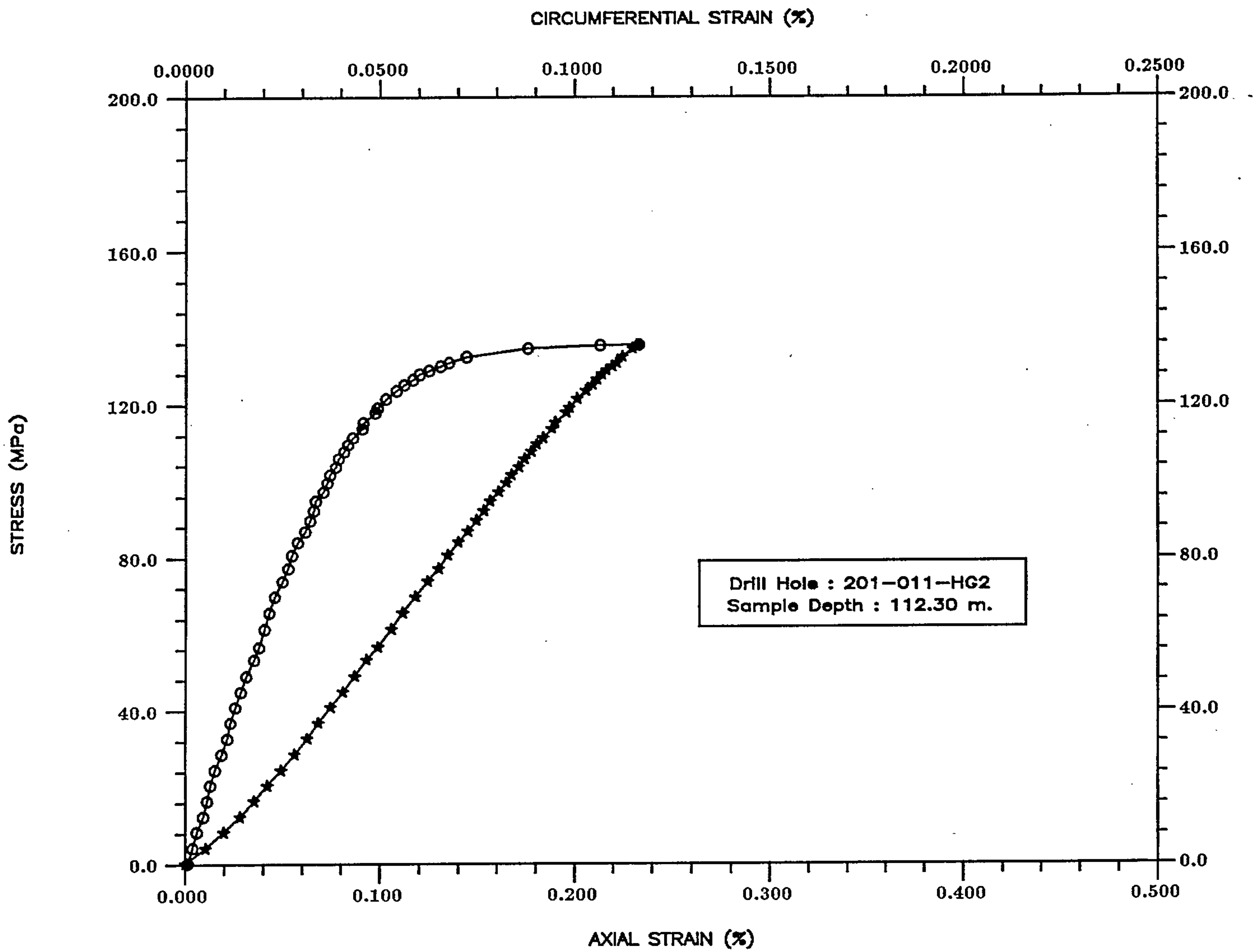

Fig. 2: Axial and circumferential stress/strain curves for anomolous uniaxial test specimens.

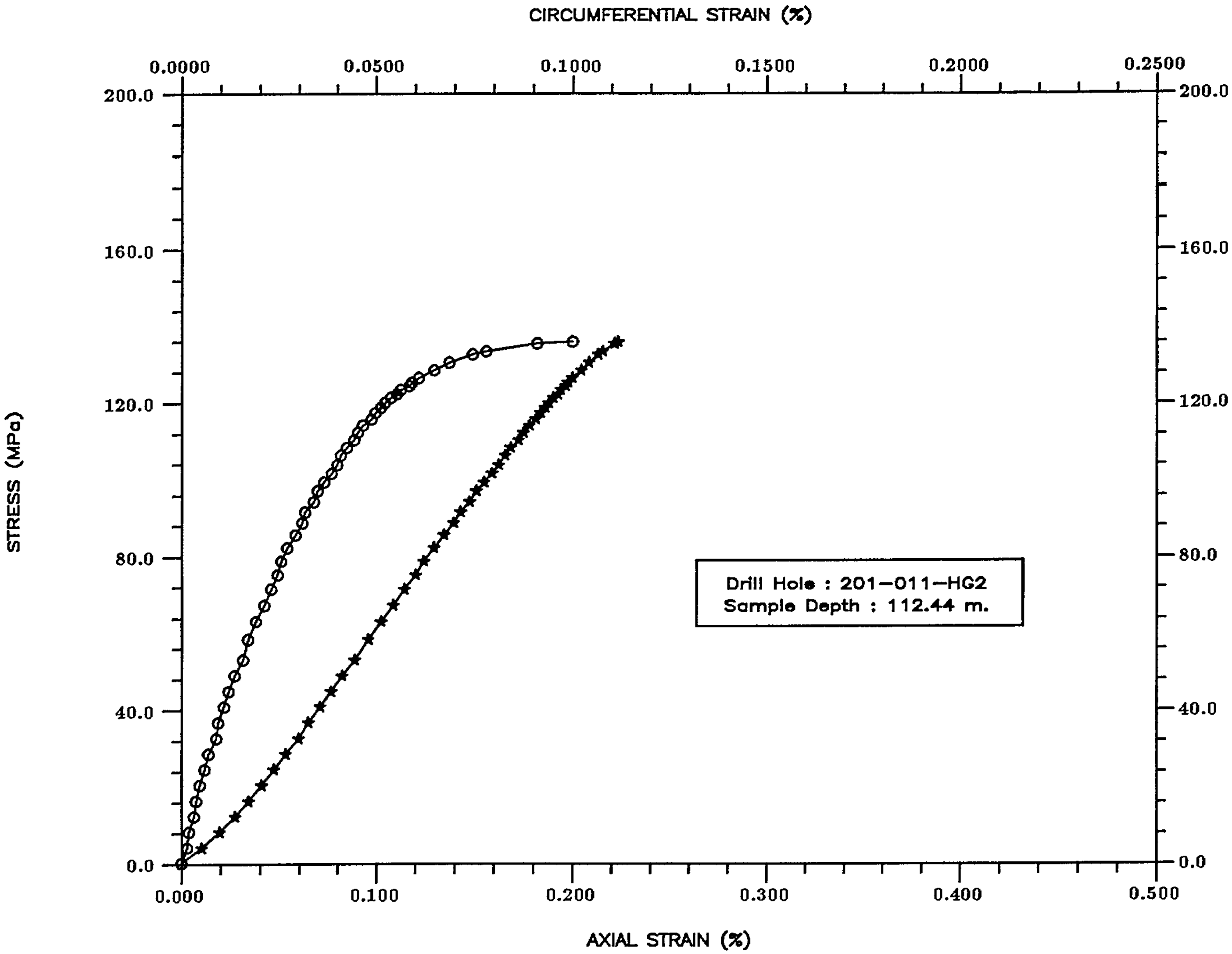

Fig. 3: Axial and circumferential stress/strain curves for anomolous uniaxial test specimens.

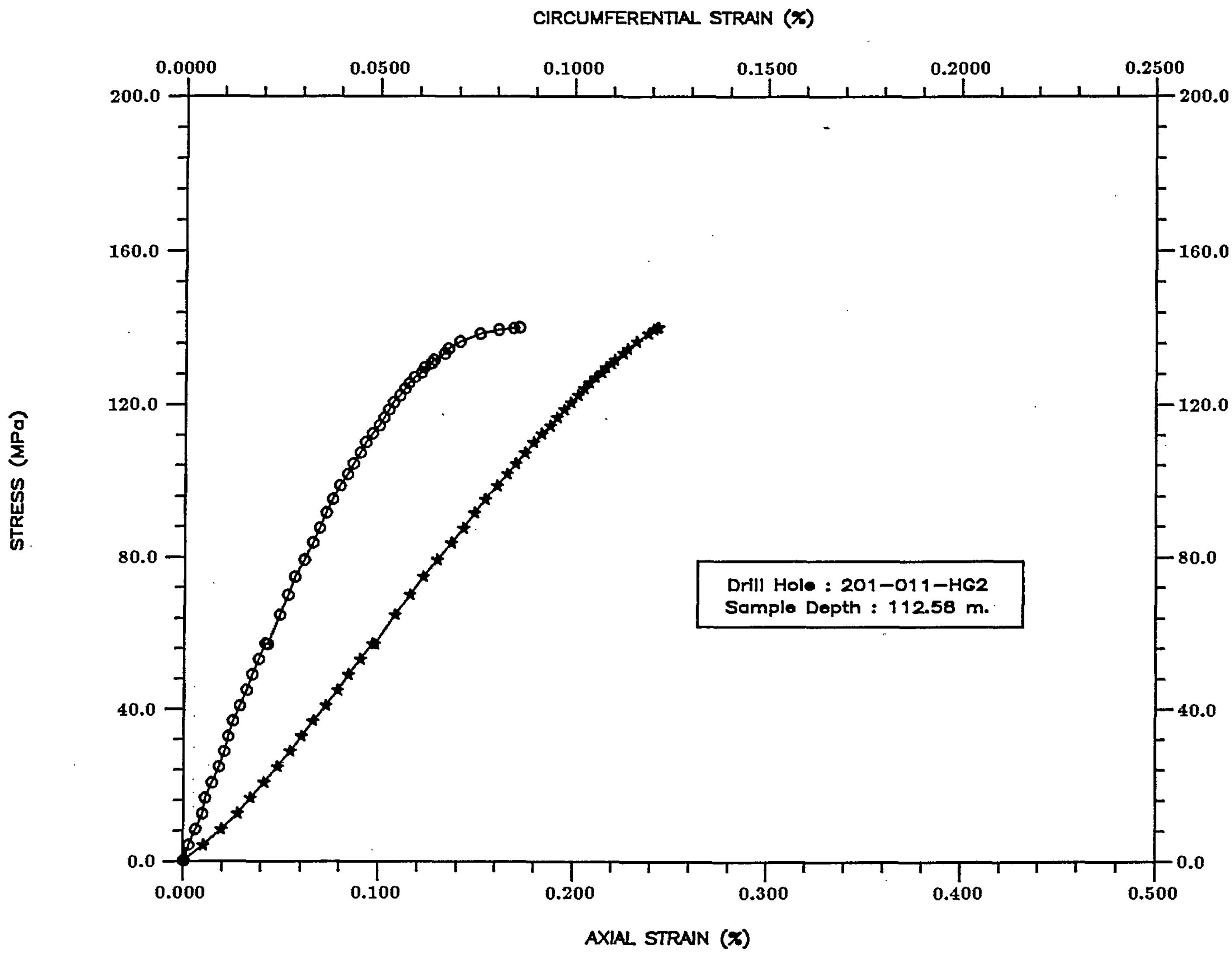

Fig. 4: Axial and circumferential stress/strain curves for anomolous uniaxial test specimens.

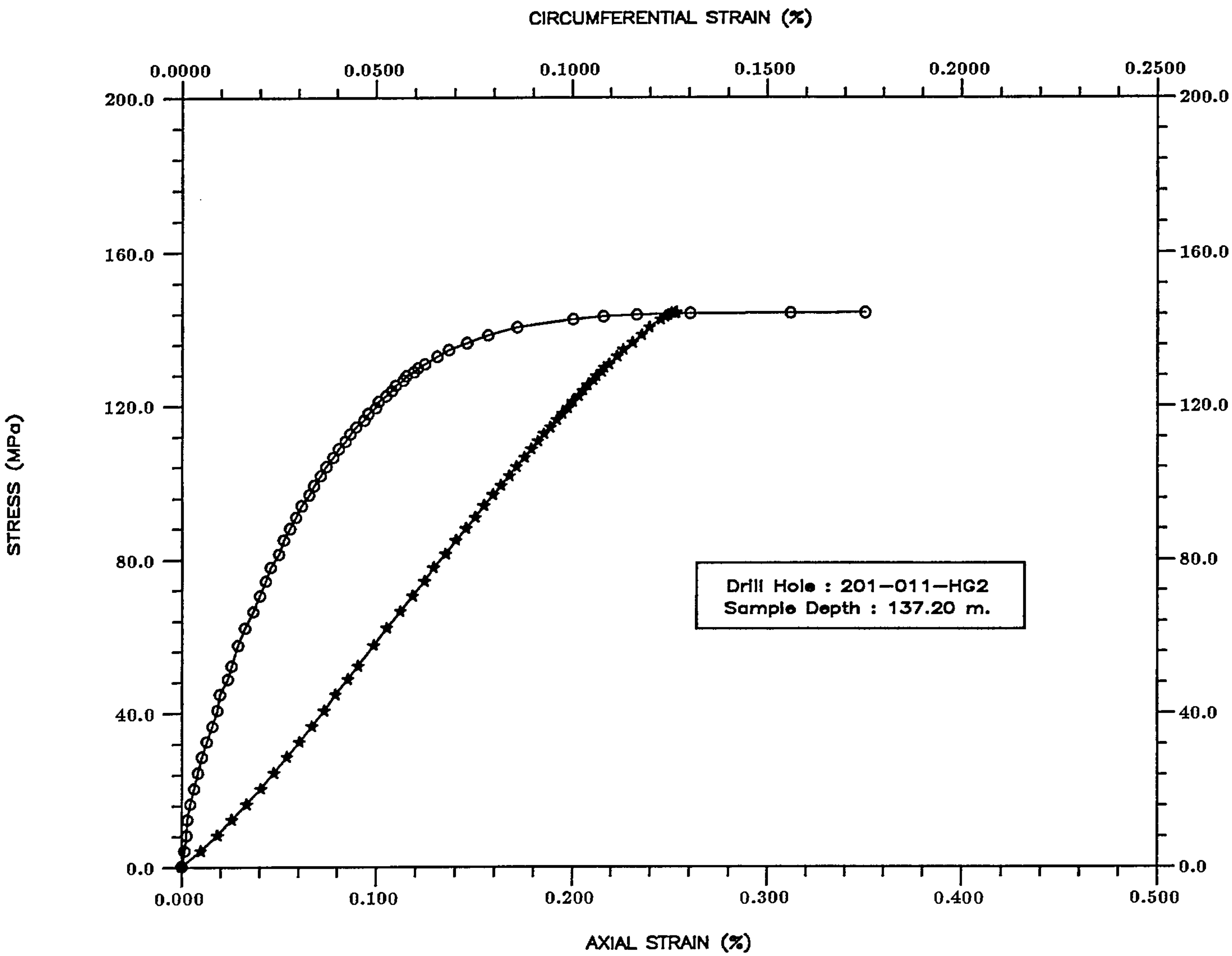

Fig. 5: Axial and circumferential stress/strain curves for anomolous uniaxial test specimens.

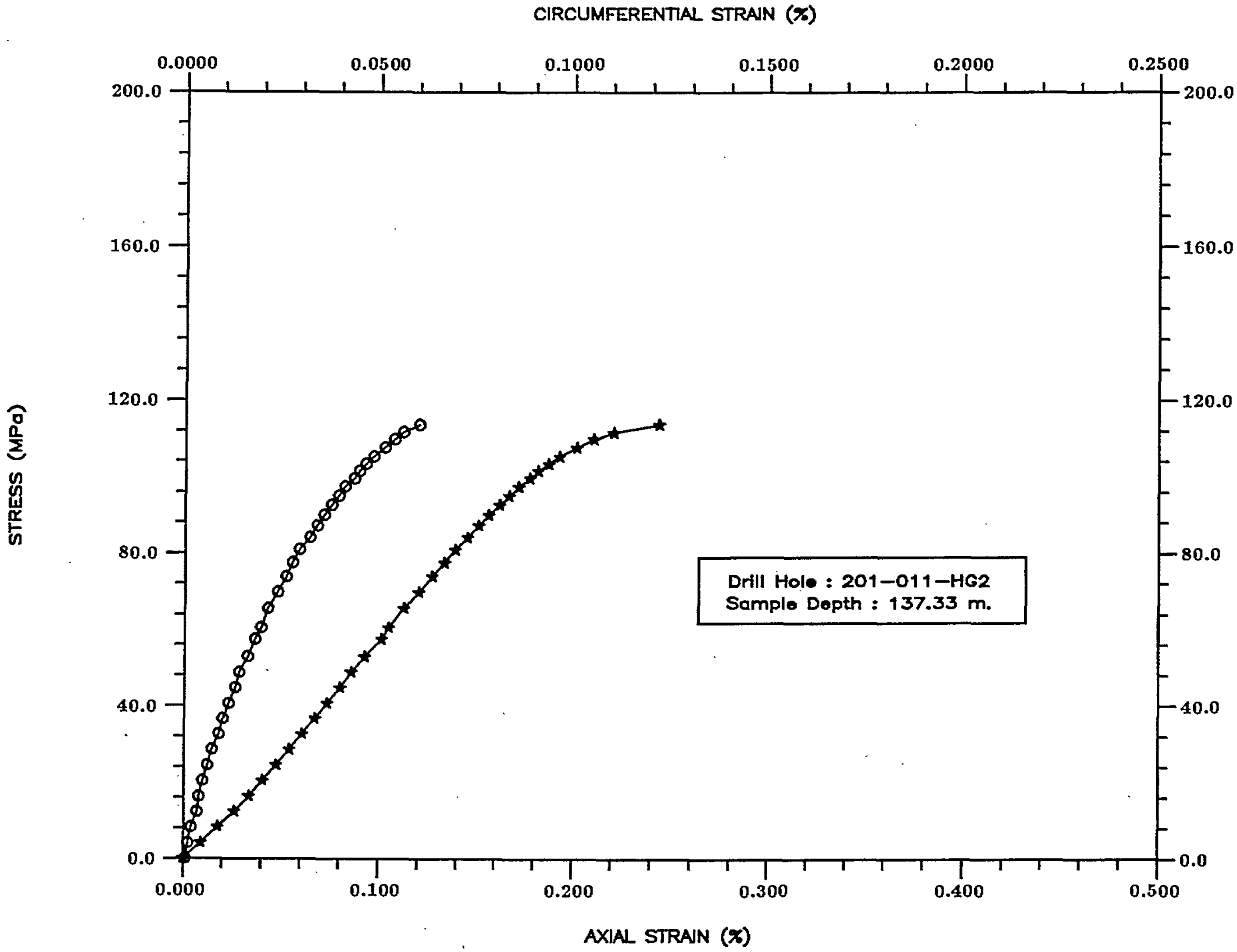

Fig. 6: Axial and circumferential stress/strain curves for anomolous uniaxial test specimens.

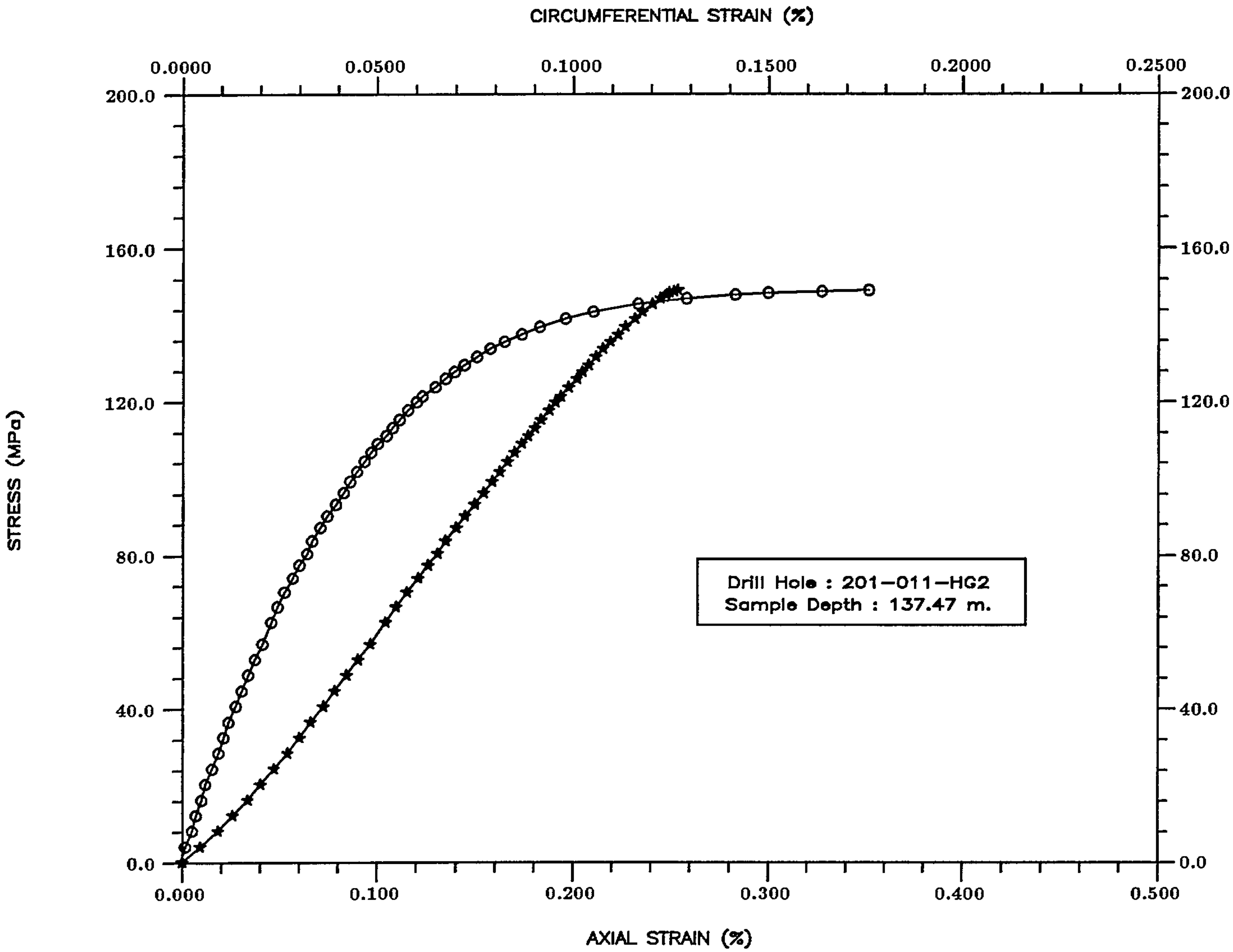

Fig. 7: Axial and circumferential stress/strain curves for anomolous uniaxial test specimens.

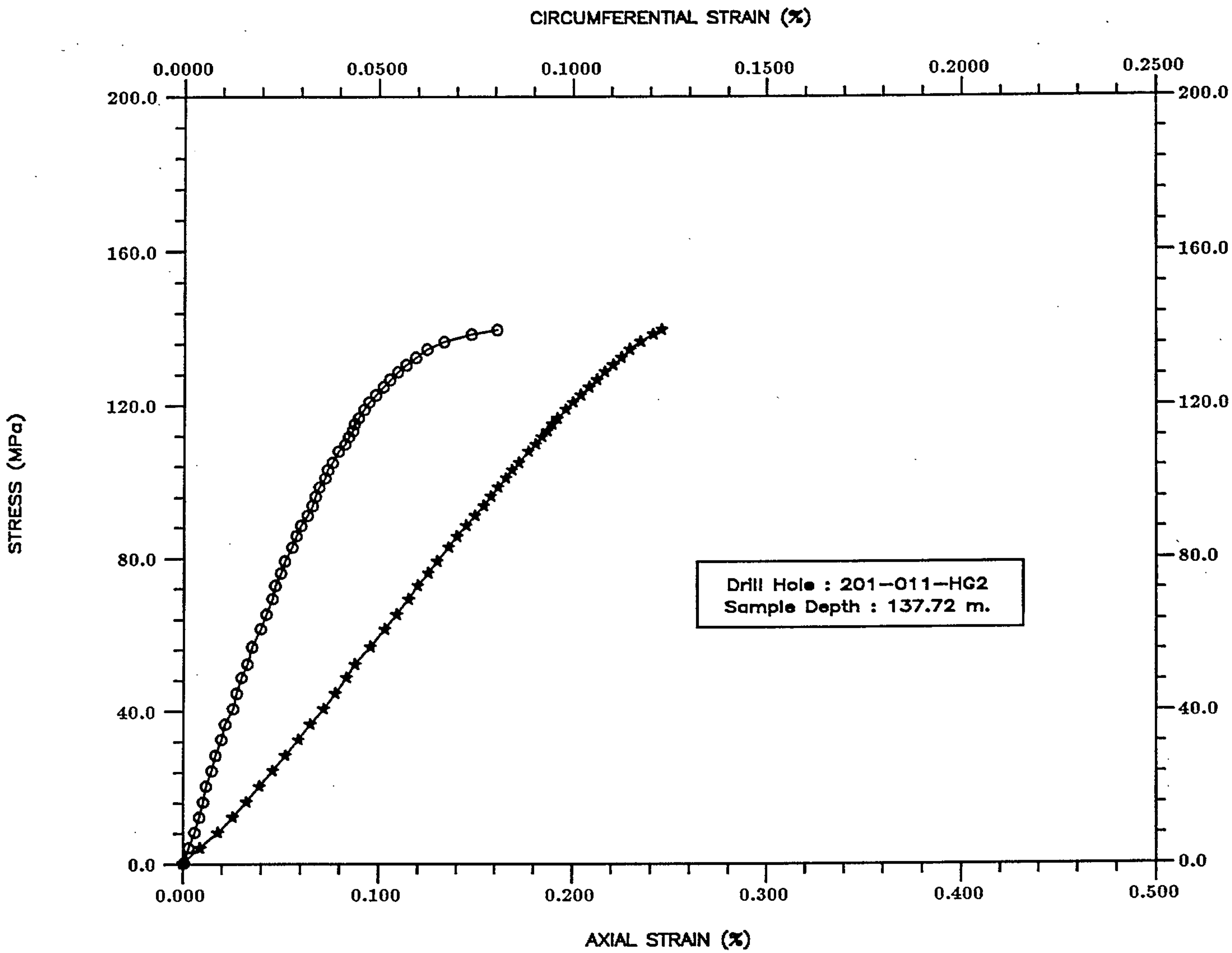

Fig. 8: Axial and circumferential stress/strain curves for anomolous uniaxial test specimens.

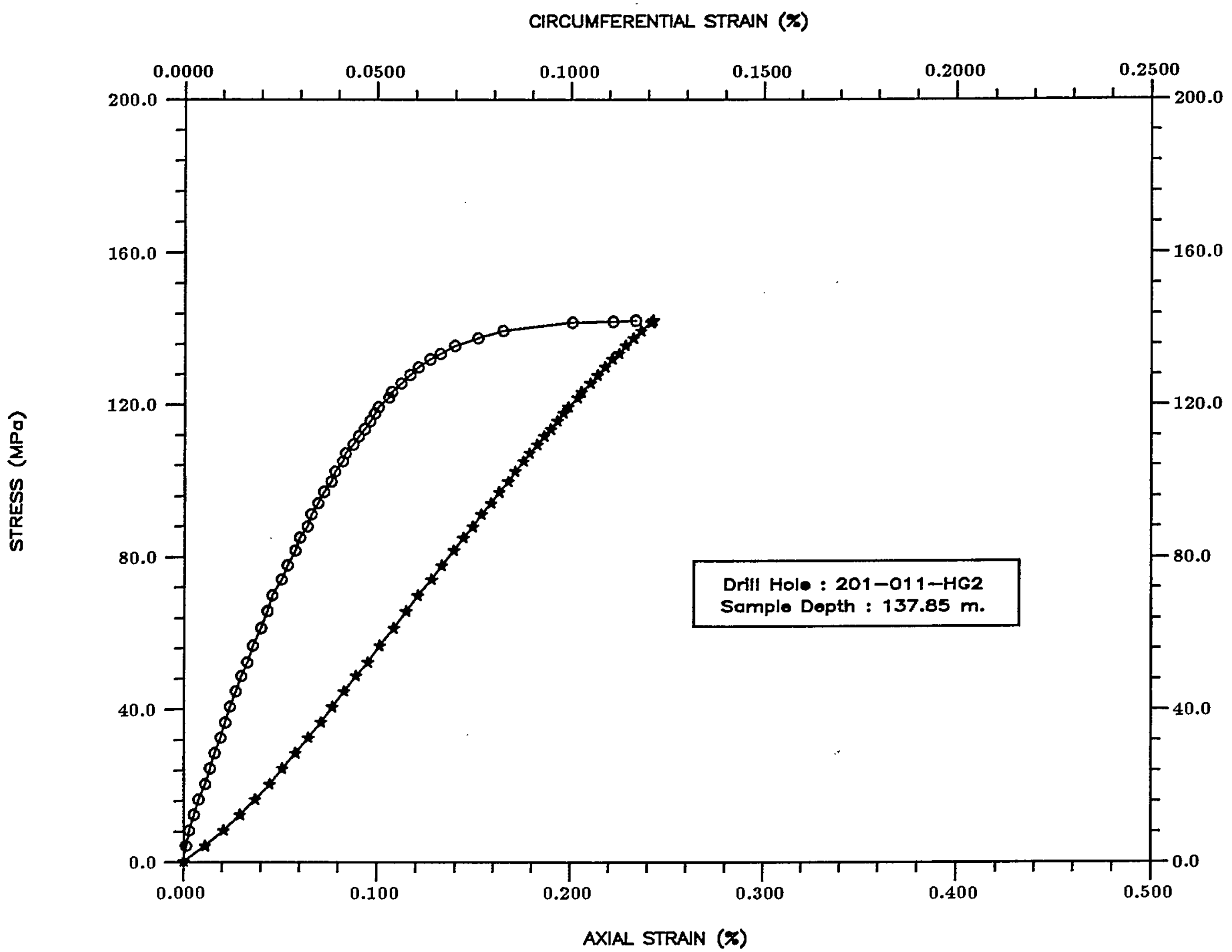

Fig. 9: Axial and circumferential stress/strain curves for anomolous uniaxial test specimens.

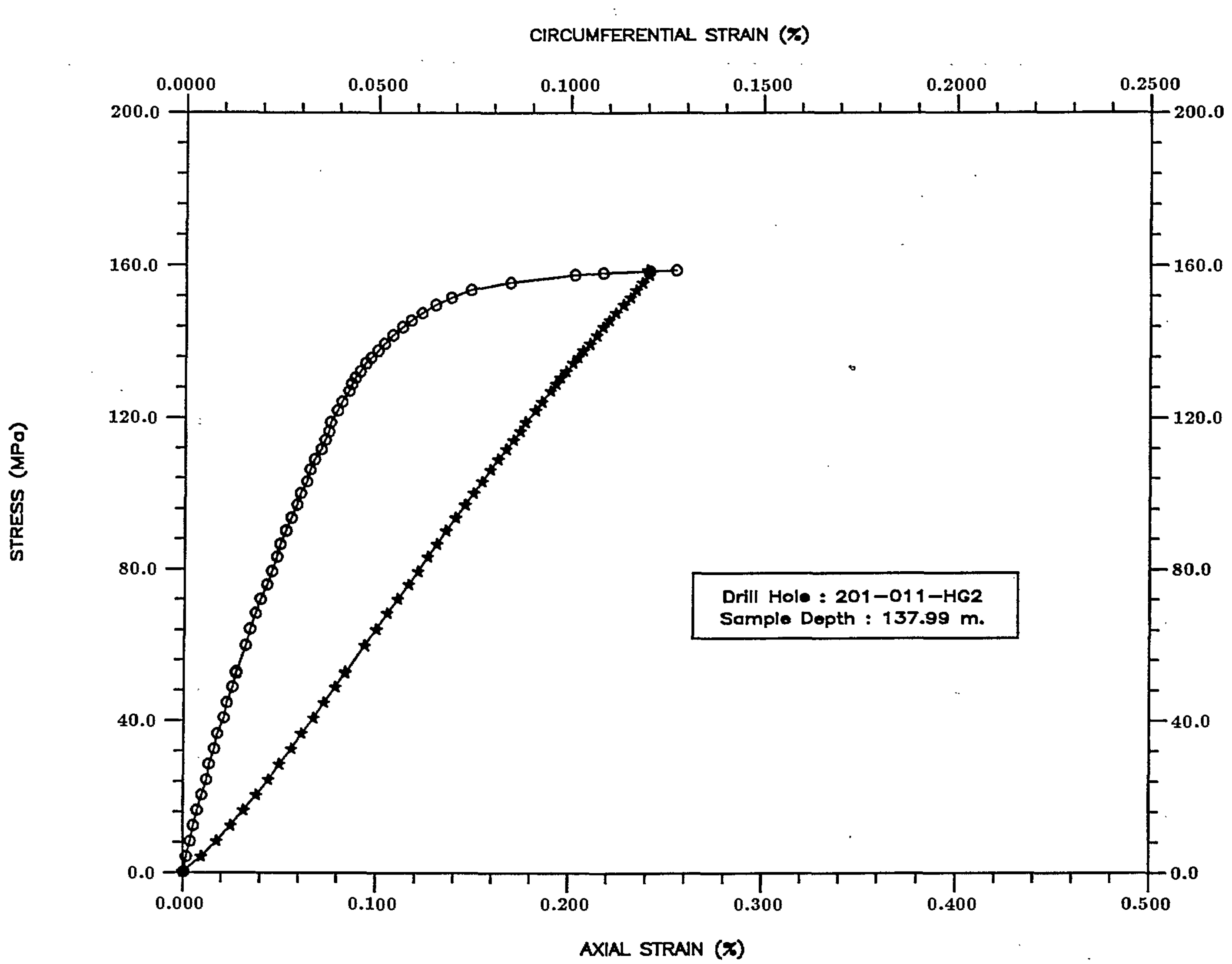

Fig. 10: Axial and circumferential stress/strain curves for anomolous uniaxial test specimens.

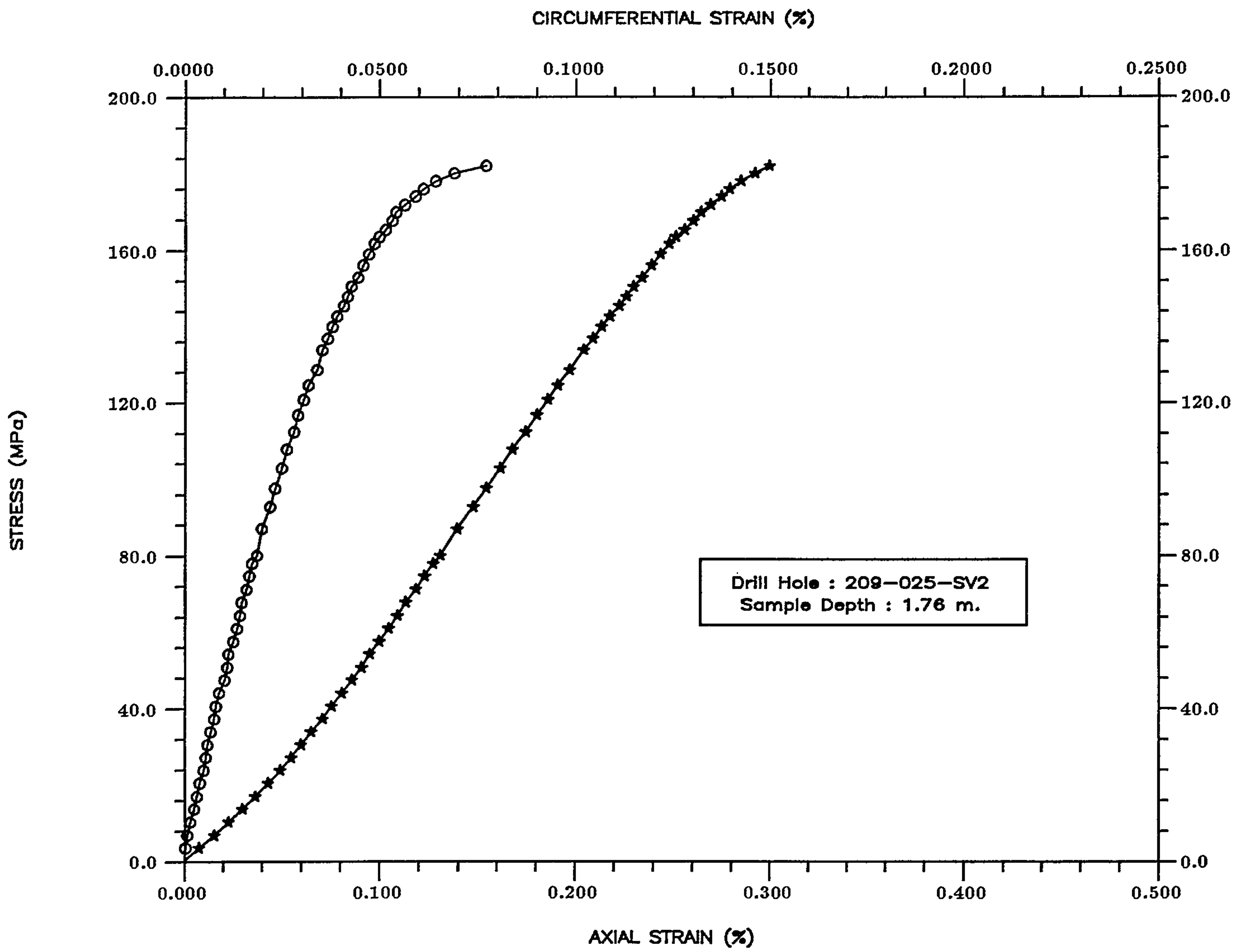

Fig. 11: Axial and circumferential stress/strain curves for anomolous uniaxial test specimens.

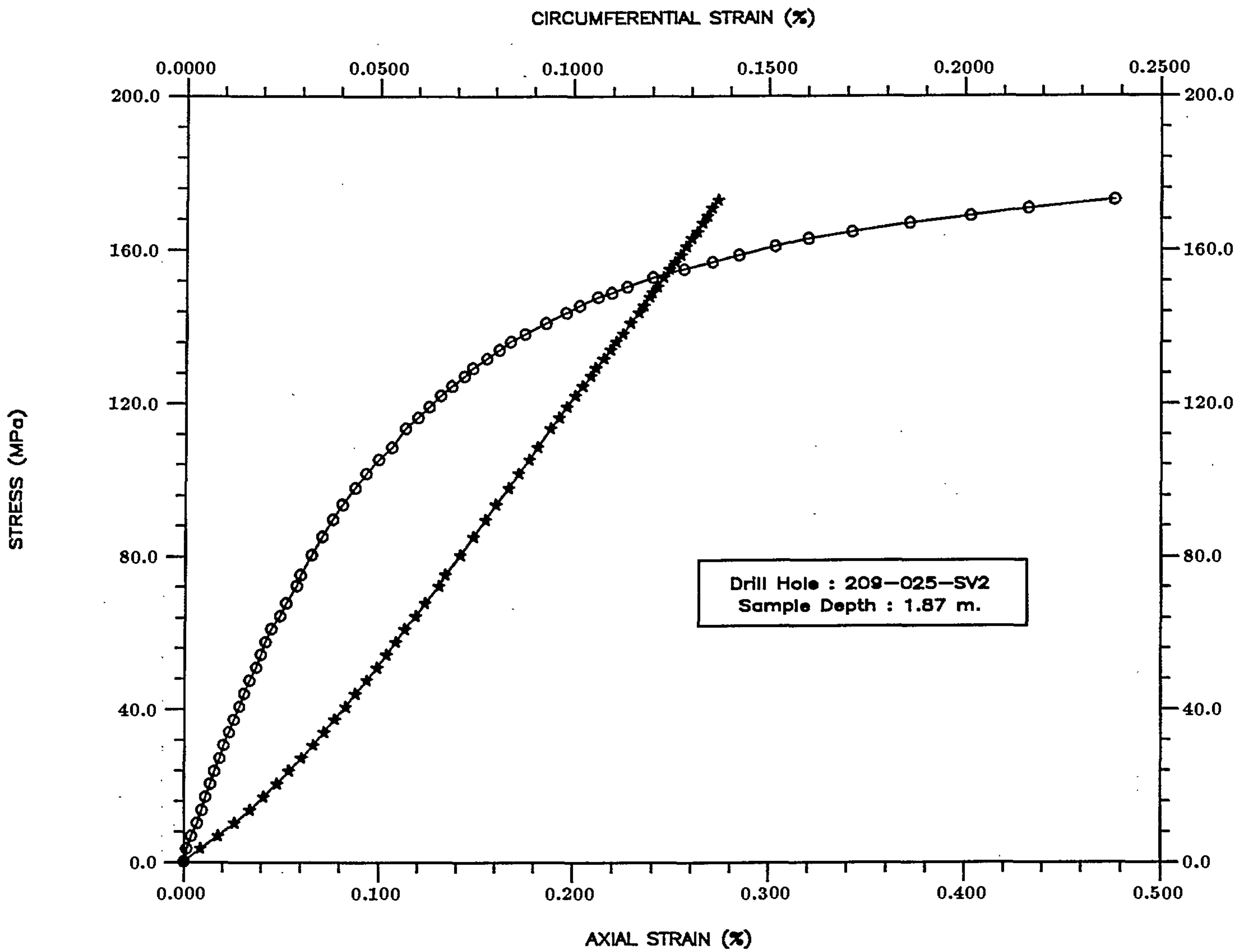

Fig. 12: Axial and circumferential stress/strain curves for anomolous uniaxial test specimens.

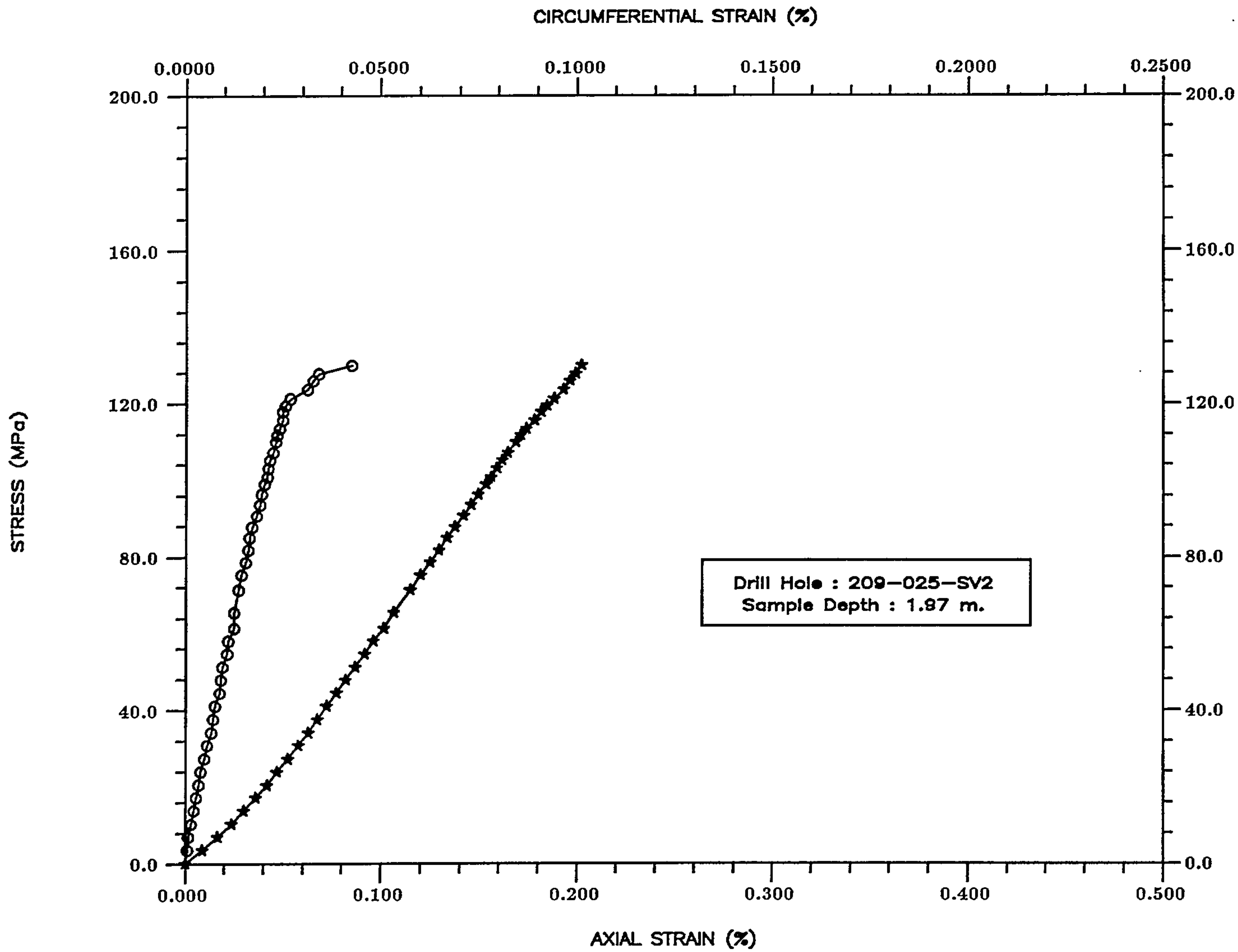

Fig. 13: Axial and circumferential stress/strain curves for anomolous uniaxial test specimens.

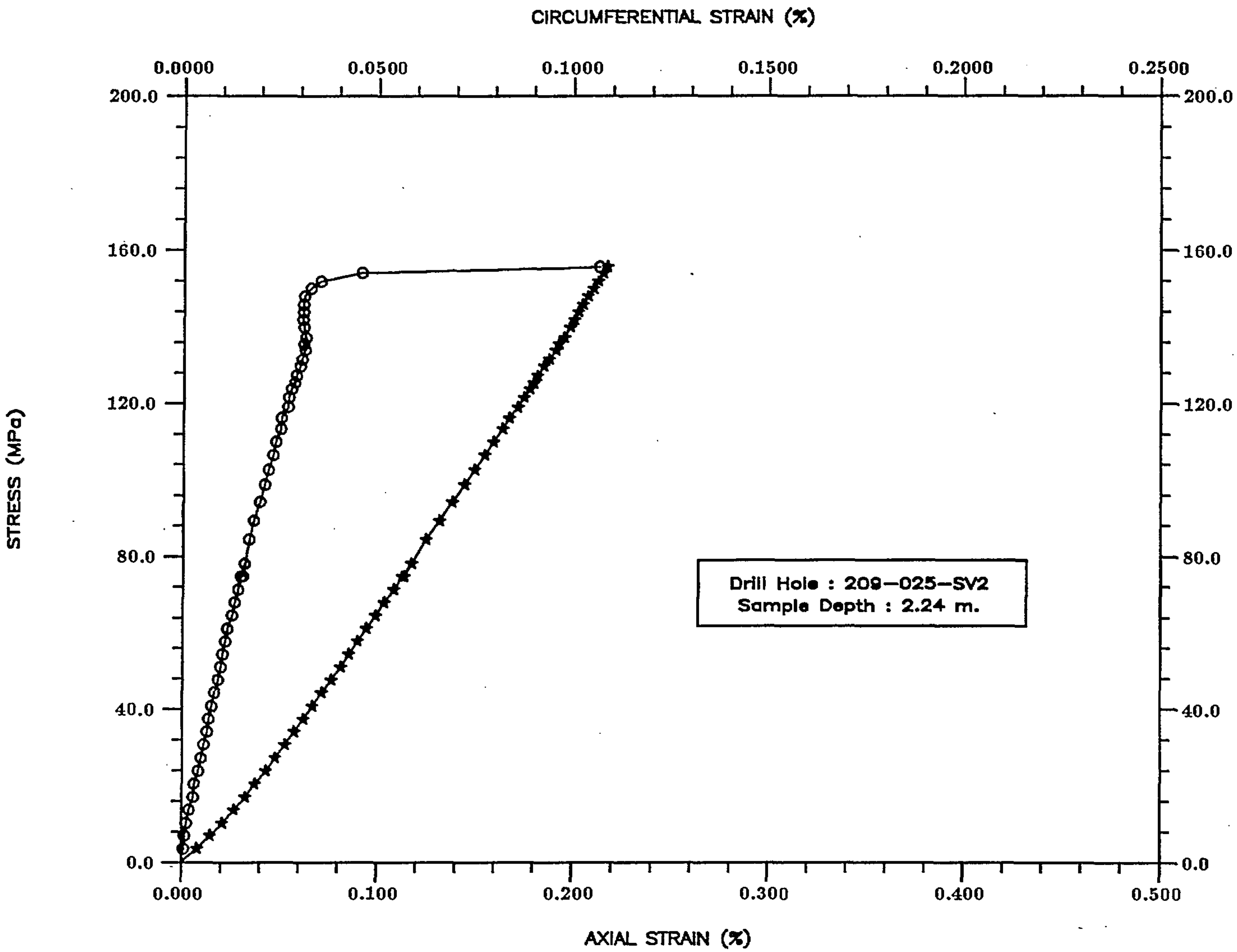

Fig. 14: Axial and circumferential stress/strain curves for anomolous uniaxial test specimens.

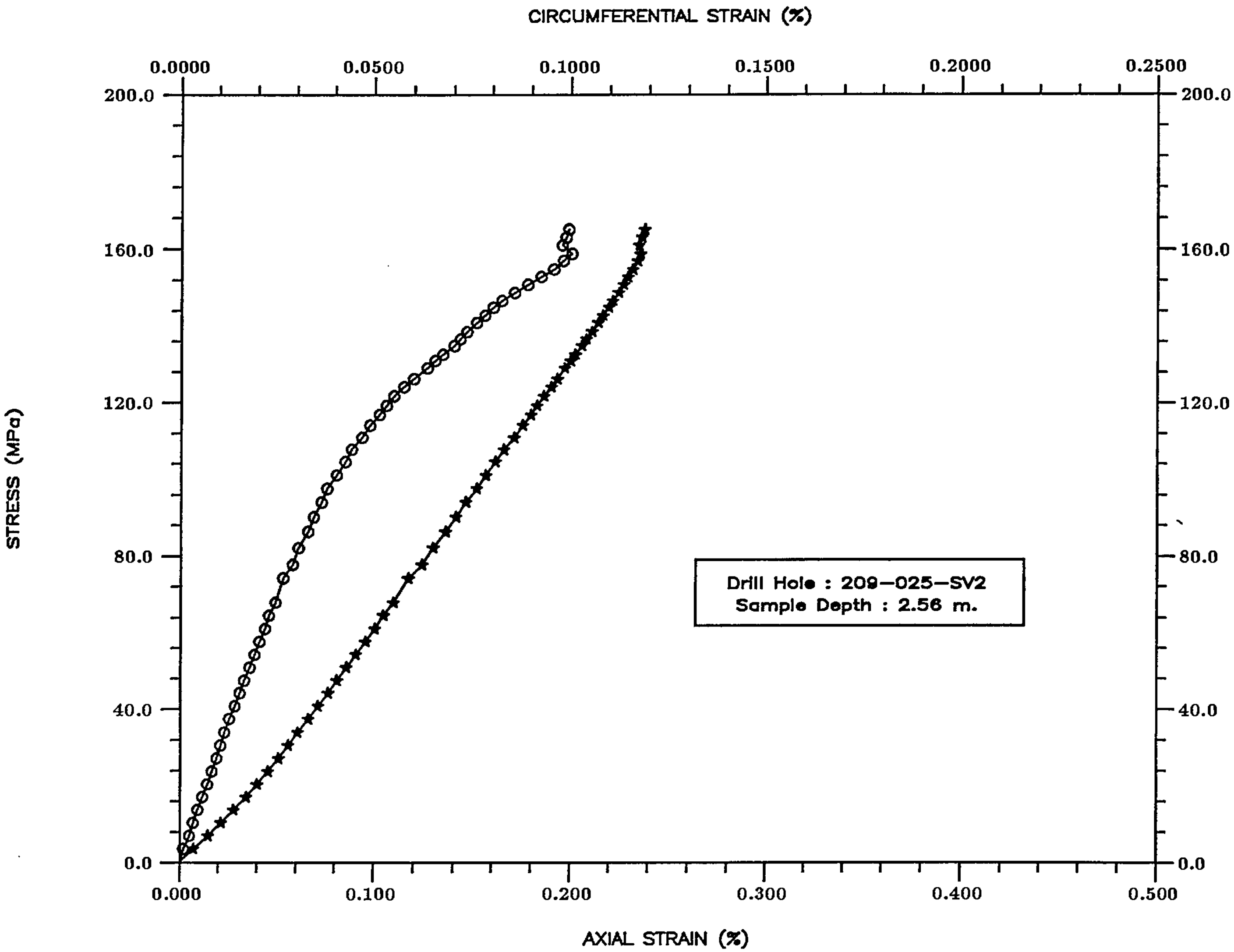

Fig. 15: Axial and circumferential stress/strain curves for anomolous uniaxial test specimens.

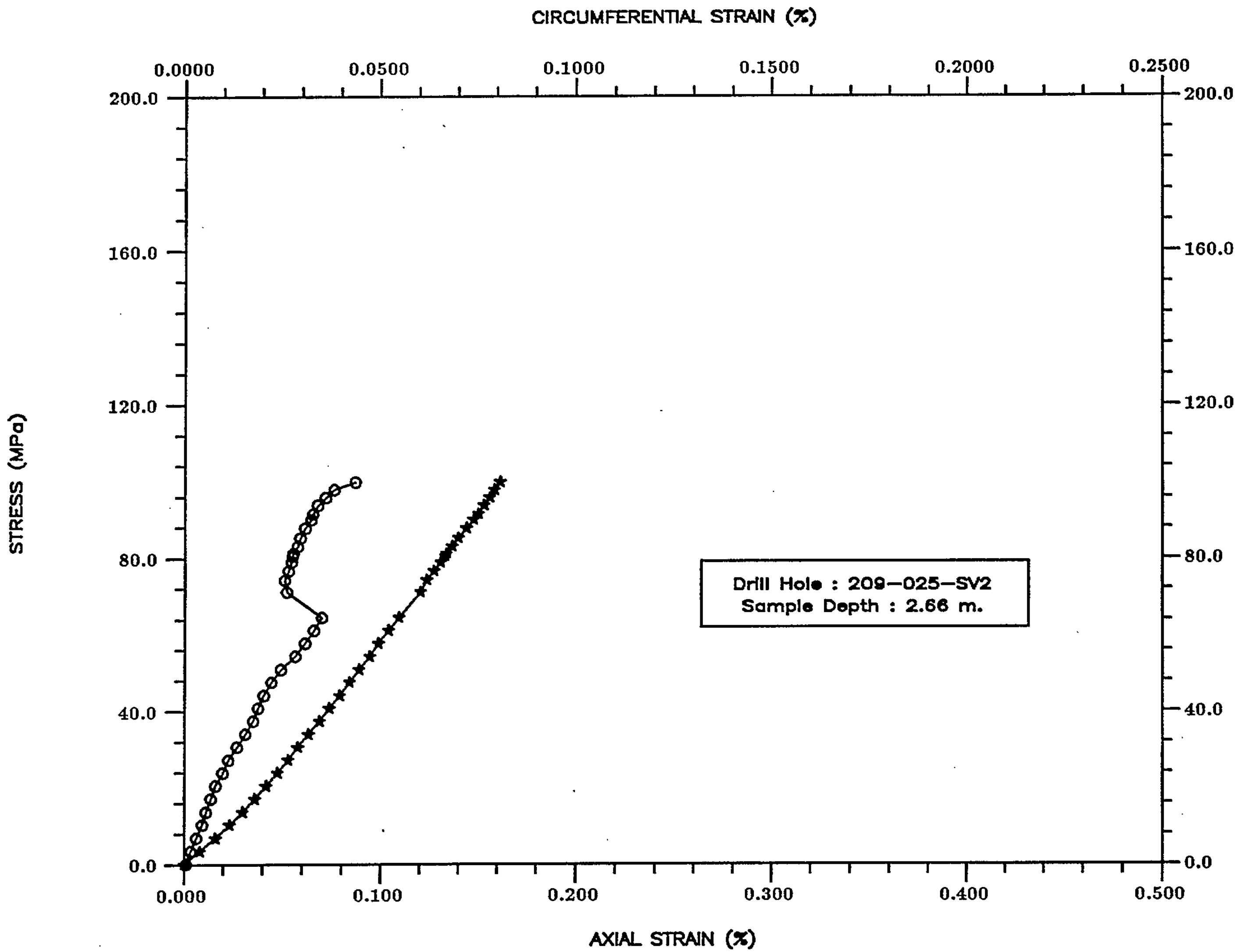

Fig. 16: Axial and circumferential stress/strain curves for anomolous uniaxial test specimens.

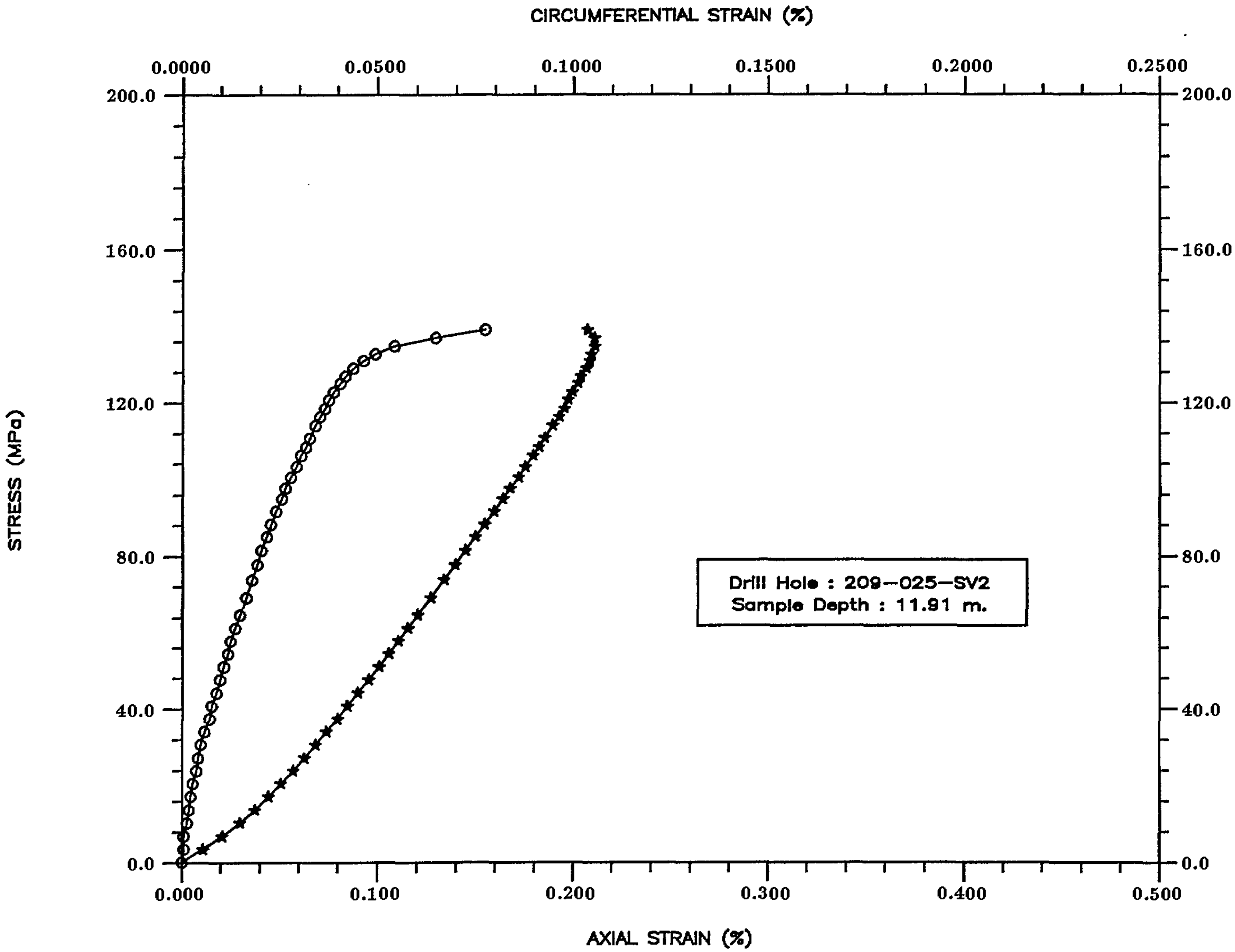

Fig. 17: Axial and circumferential stress/strain curves for anomolous uniaxial test specimens.

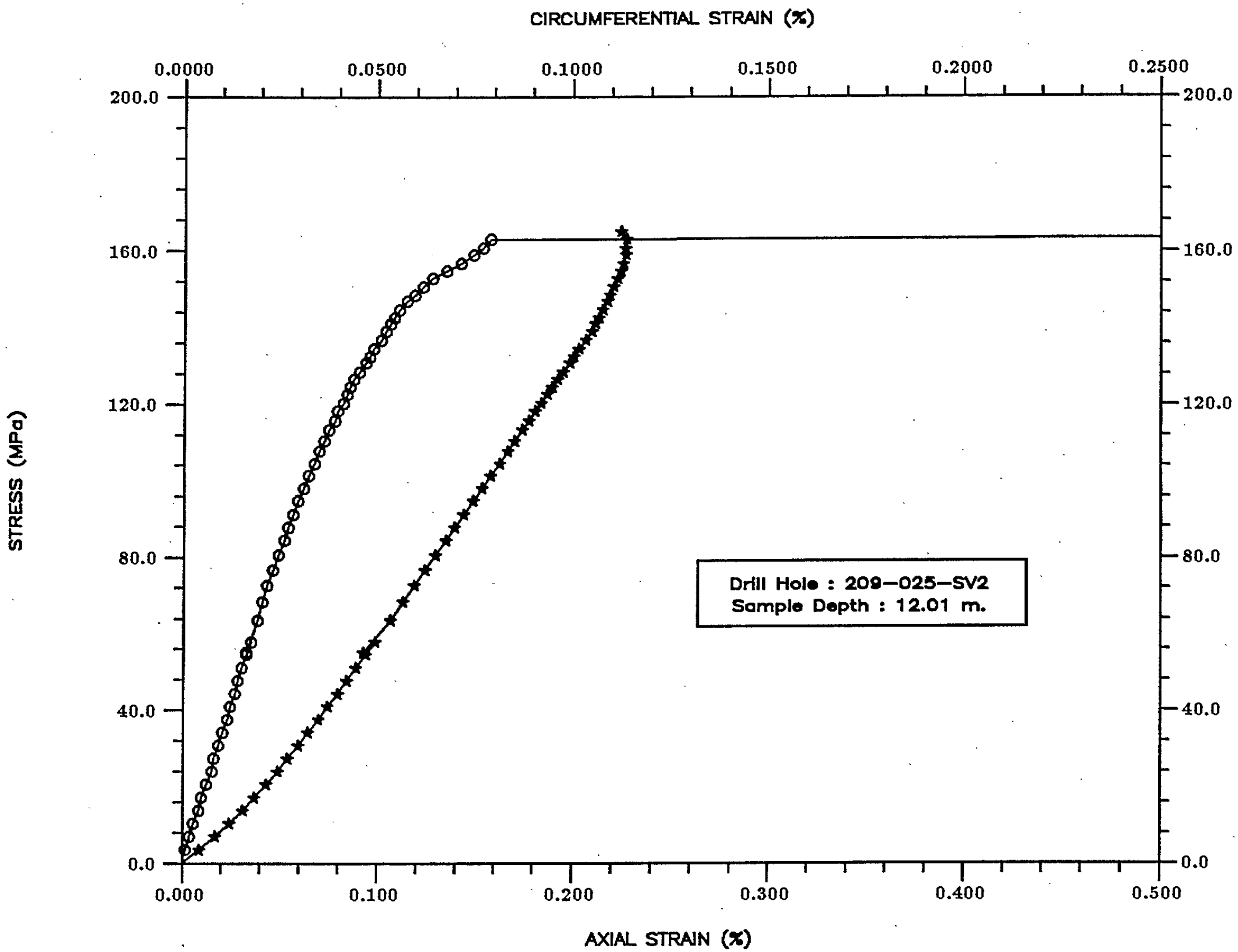

Fig. 18: Axial and circumferential stress/strain curves for anomolous uniaxial test specimens.

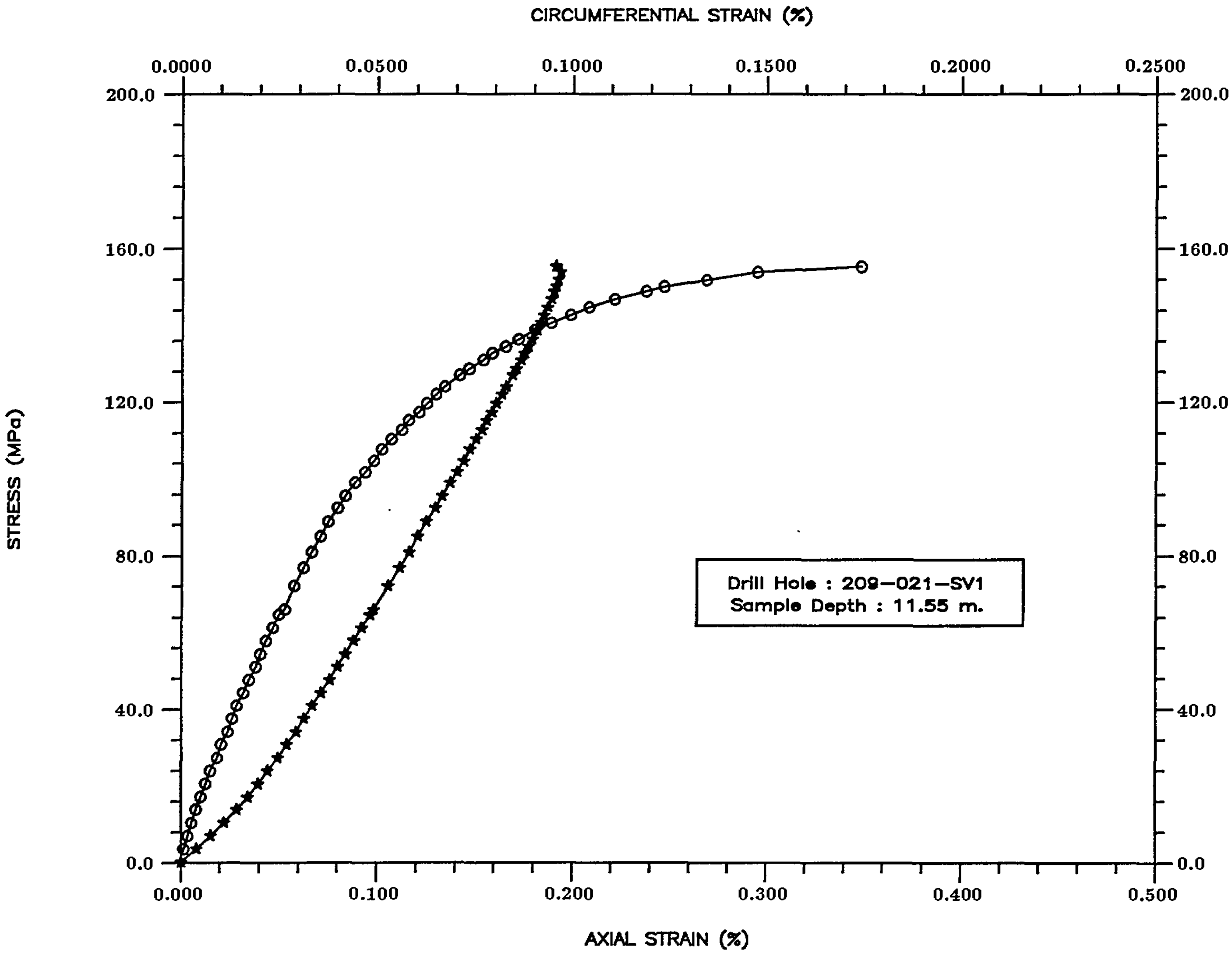

Fig. 19: Axial and circumferential stress/strain curves for anomolous uniaxial test specimens.

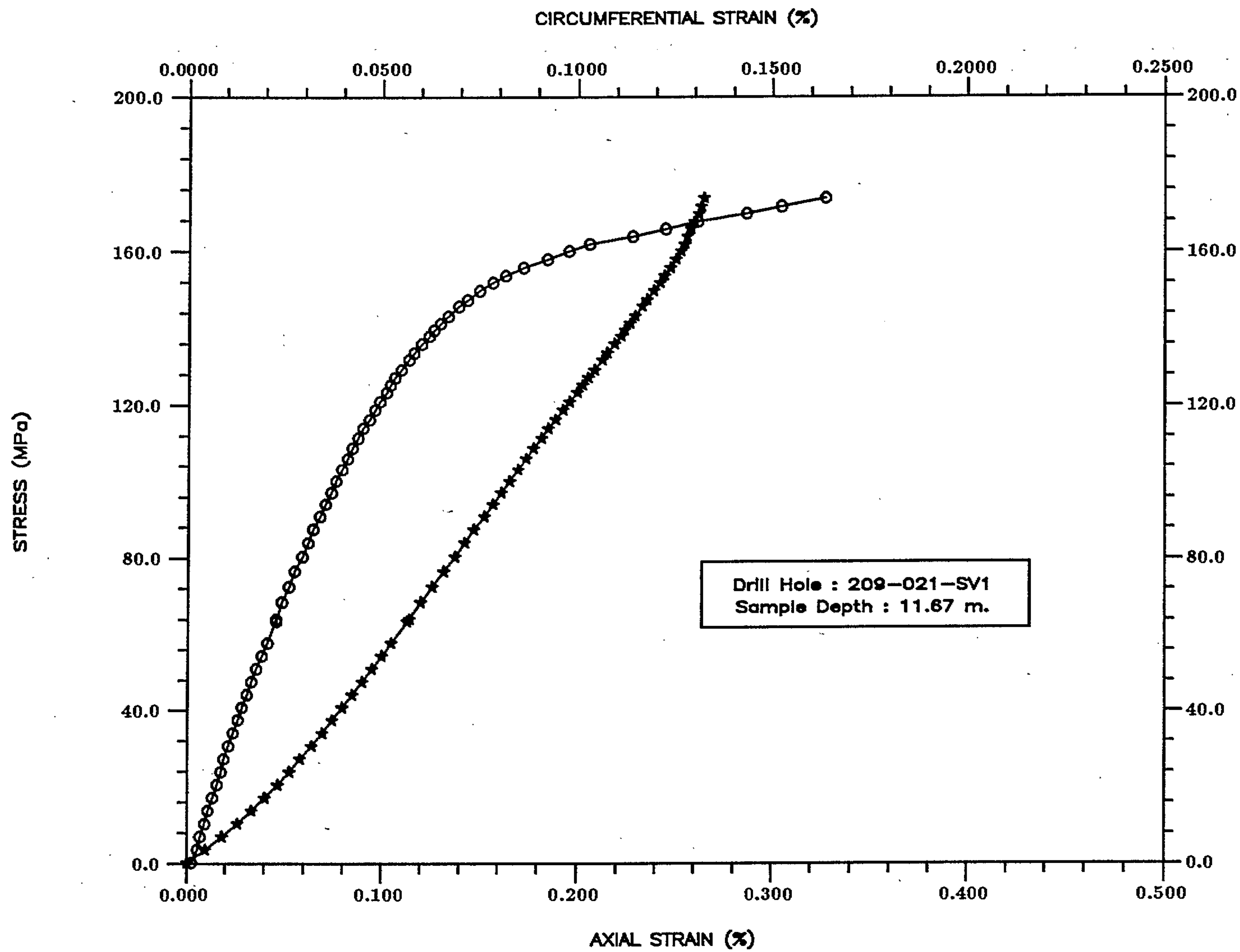

Fig. 20: Axial and circumferential stress/strain curves for anomolous uniaxial test specimens.

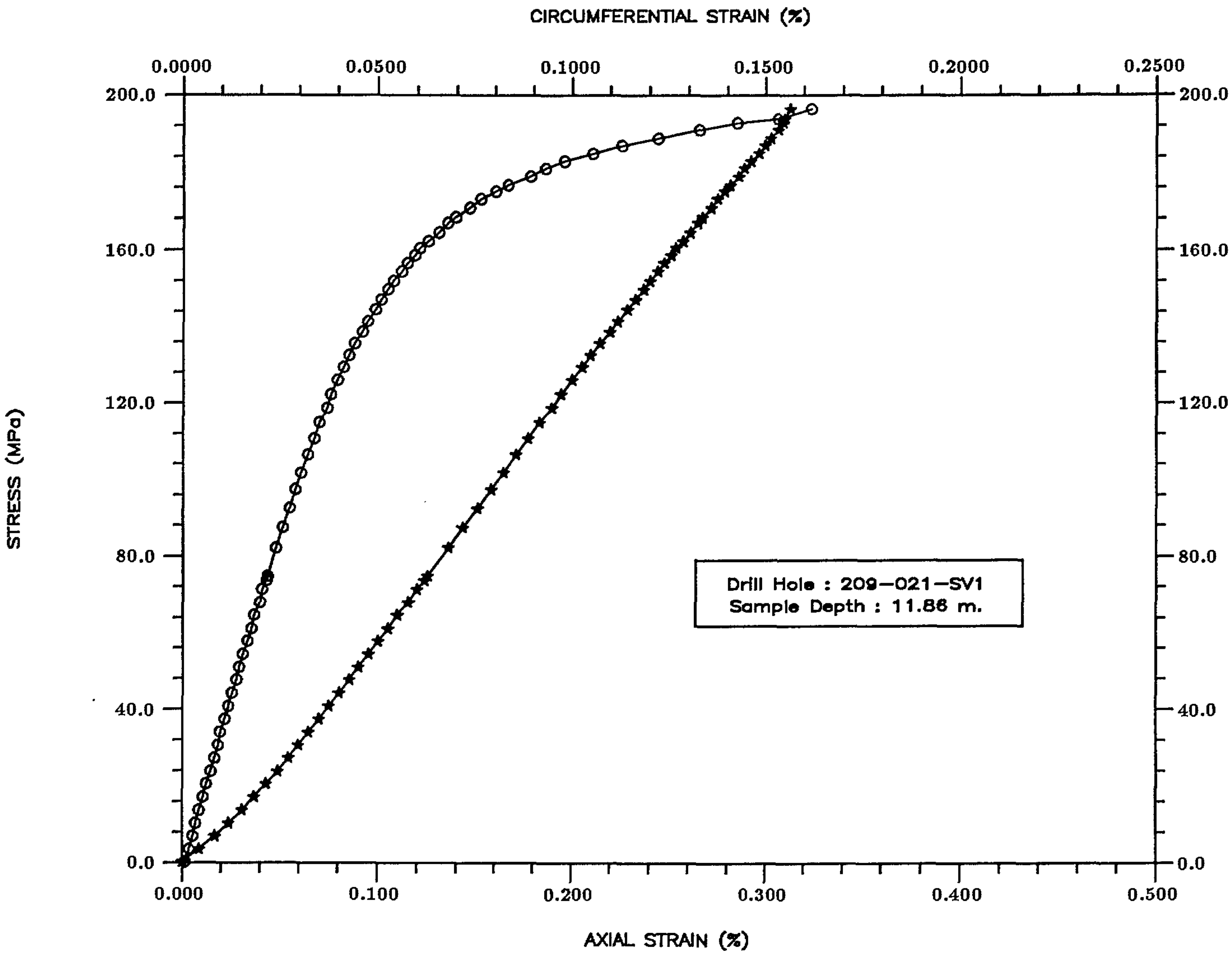

Fig. 21: Axial and circumferential stress/strain curves for anomolous uniaxial test specimens.

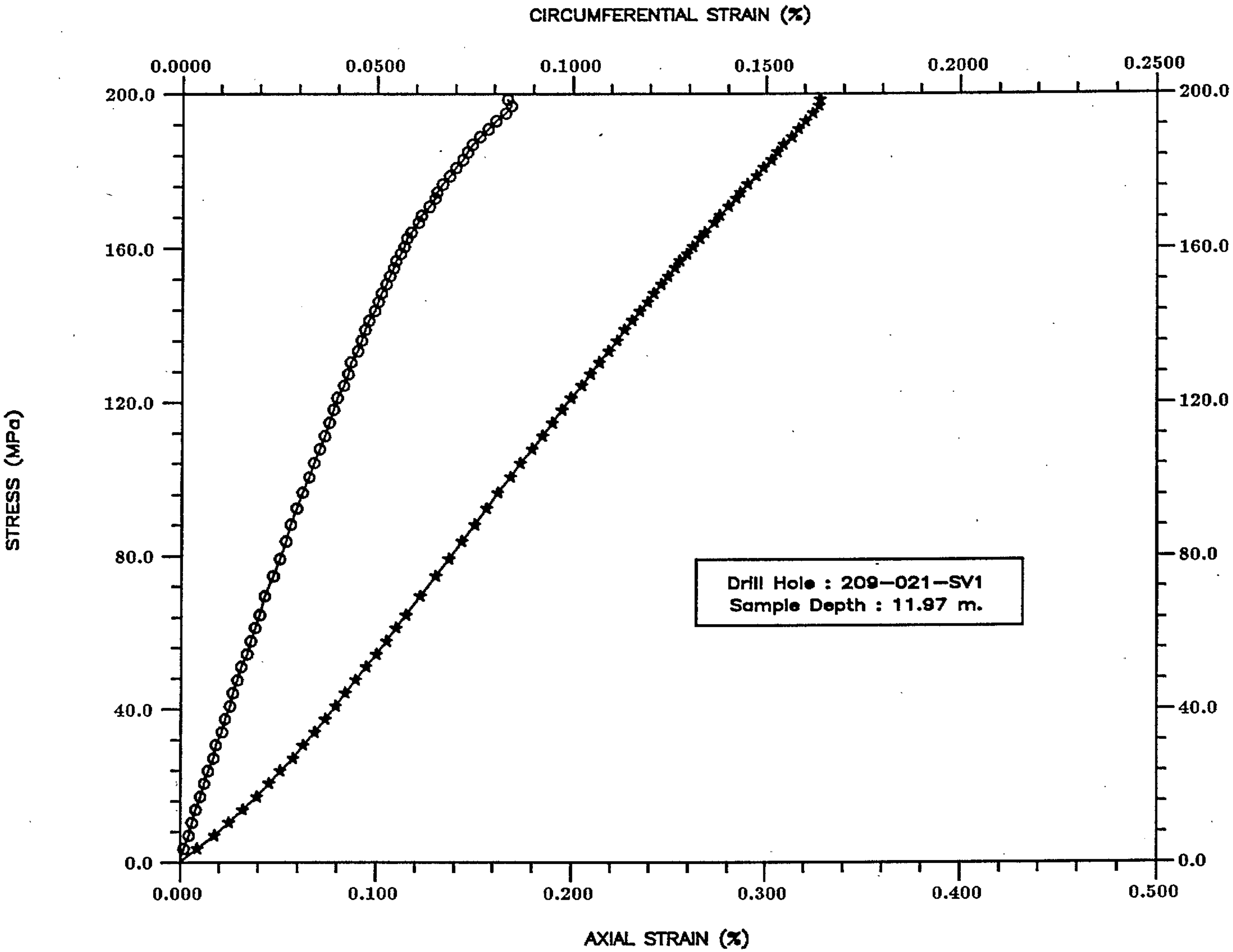

Fig. 22: Axial and circumferential stress/strain curves for anomolous uniaxial test specimens.

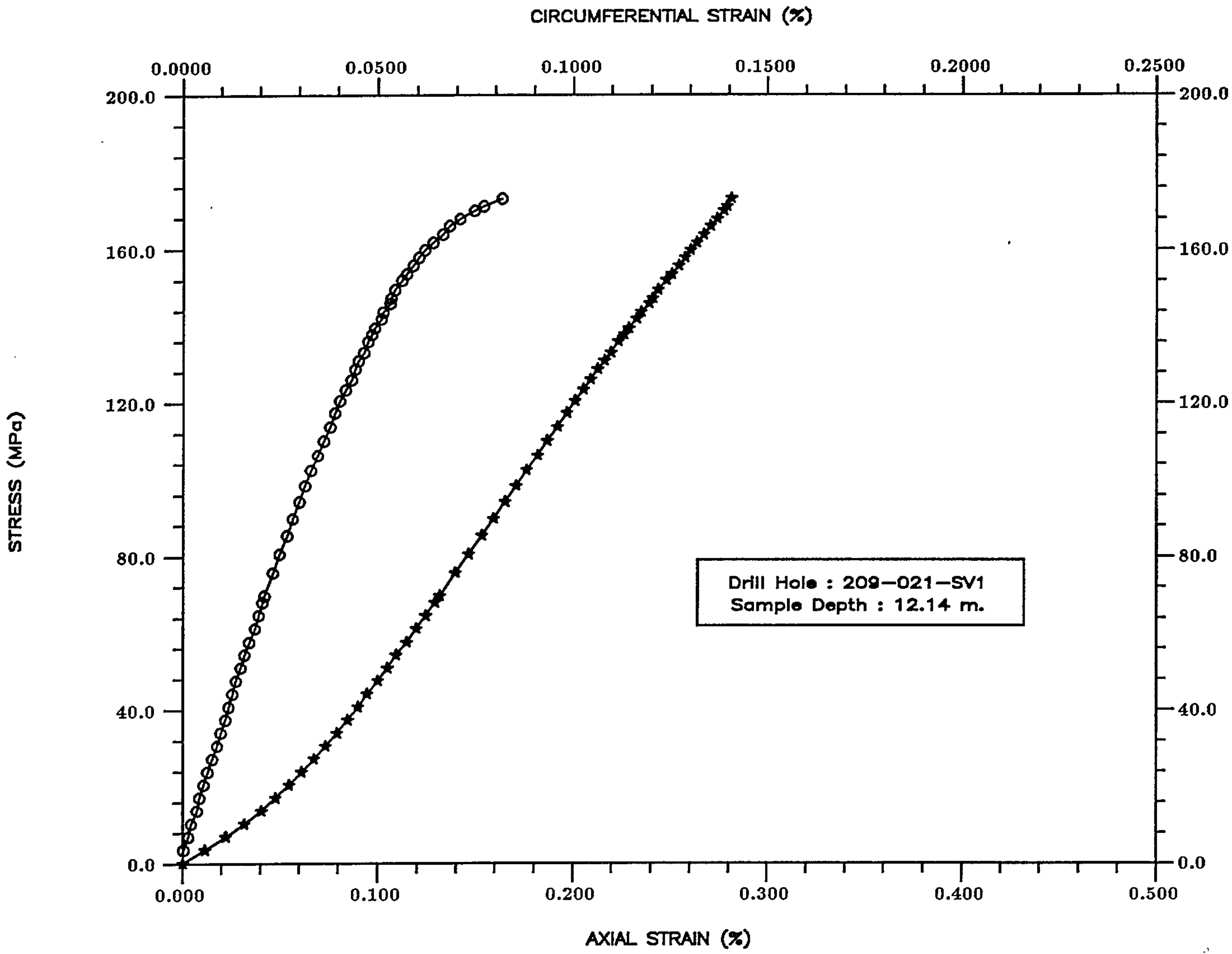

Fig. 23: Axial and circumferential stress/strain curves for anomolous uniaxial test specimens.

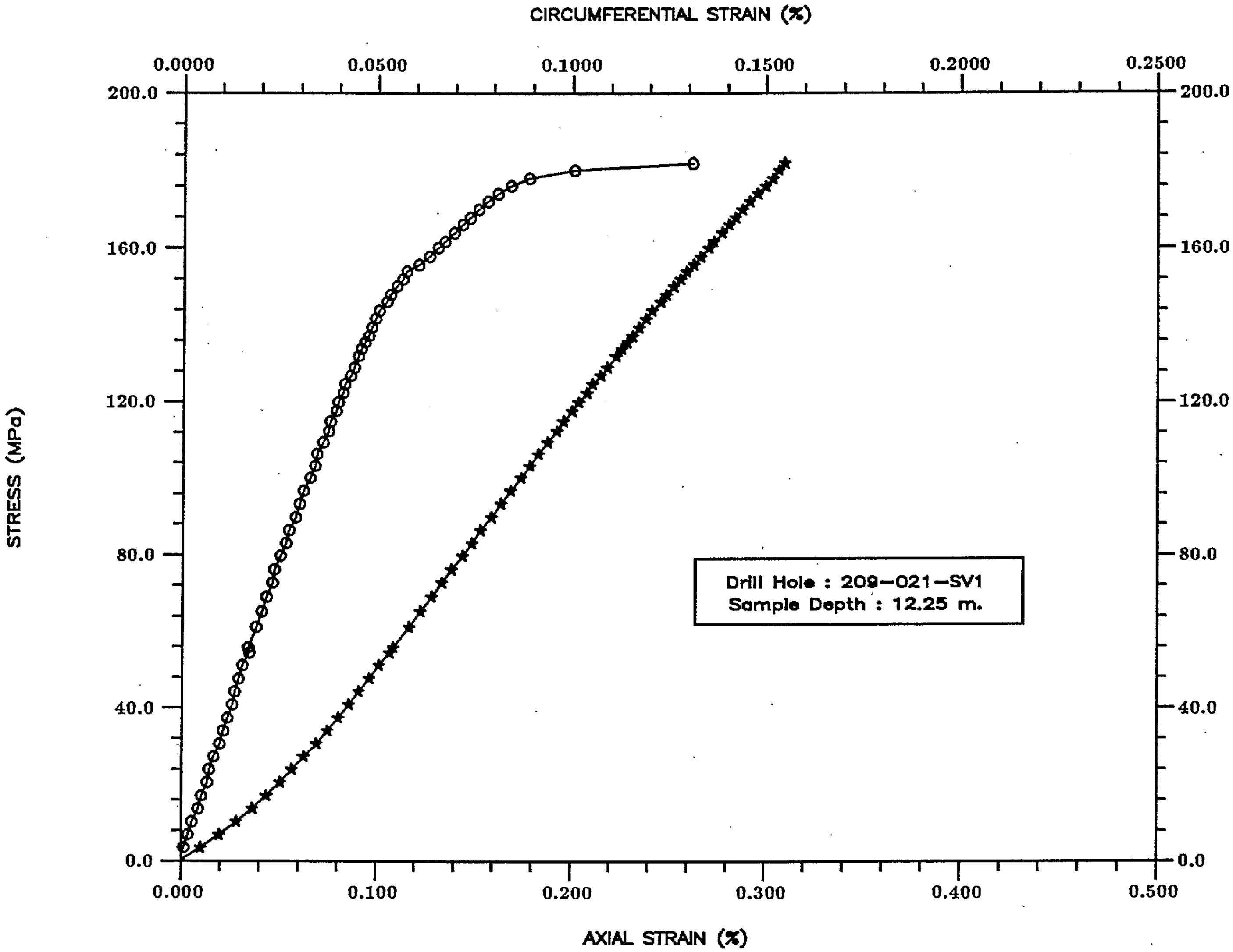

Fig. 24: Axial and circumferential stress/strain curves for anomolous uniaxial test specimens.

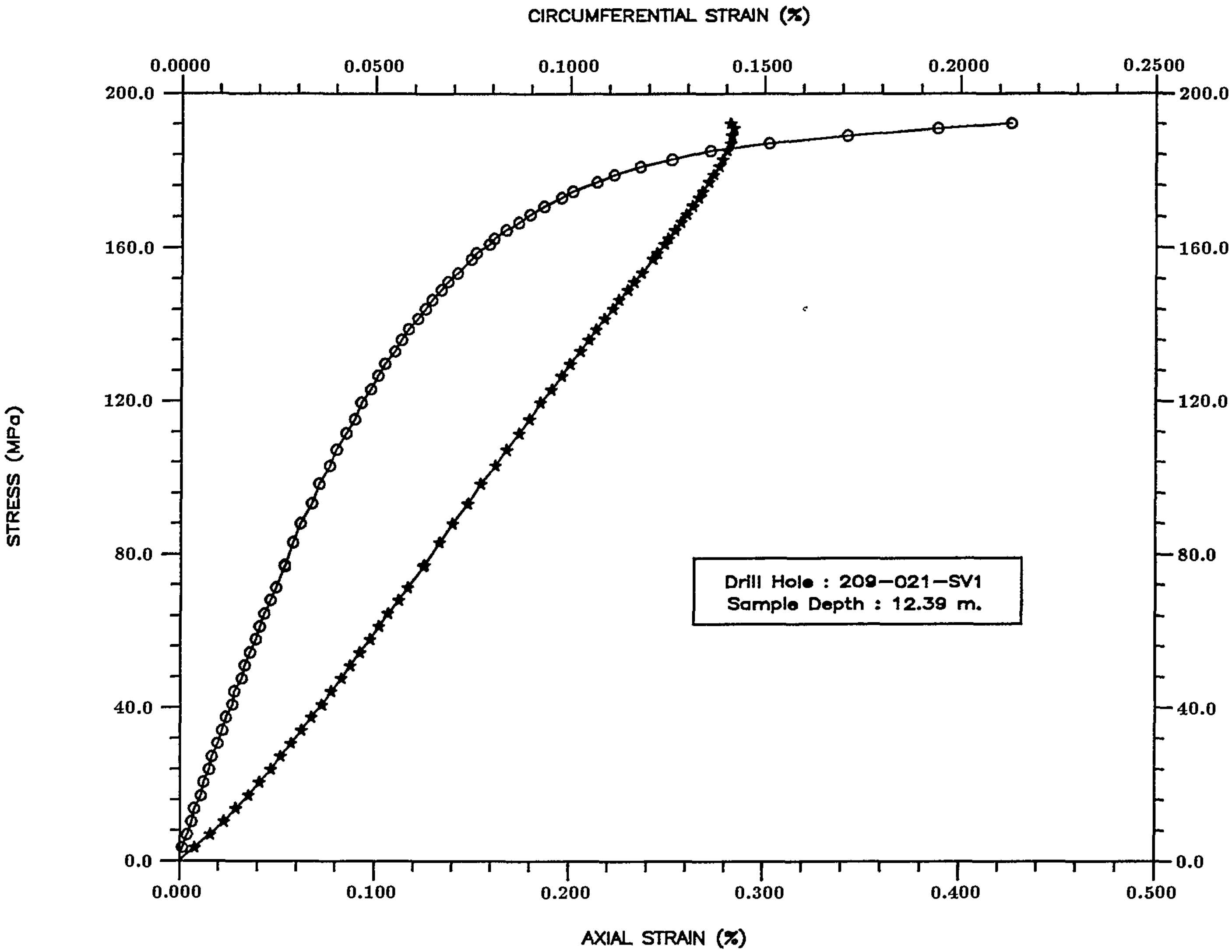

Fig. 25: Axial and circumferential stress/strain curves for anomolous uniaxial test specimens.

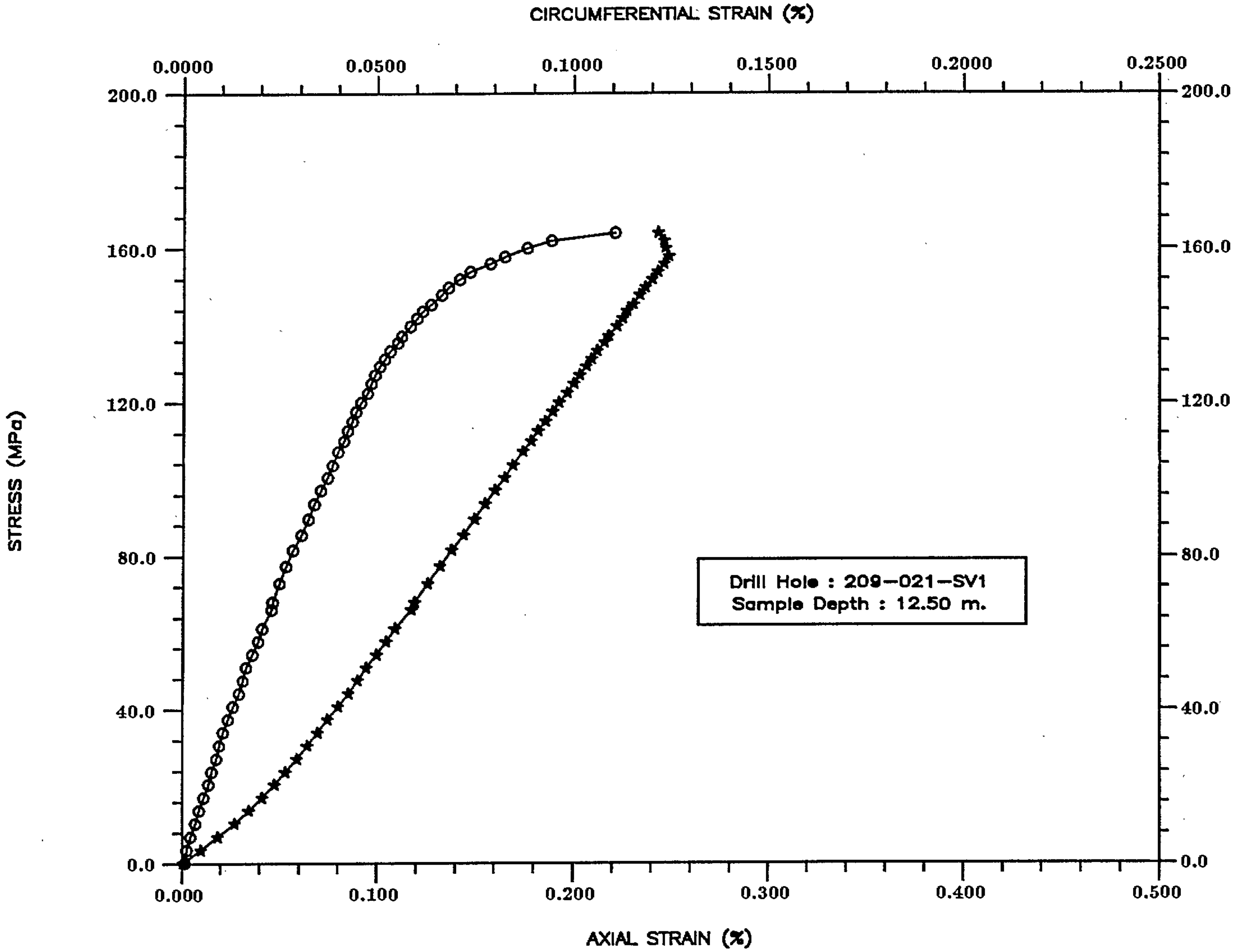

Fig. 26: Axial and circumferential stress/strain curves for anomolous uniaxial test specimens.

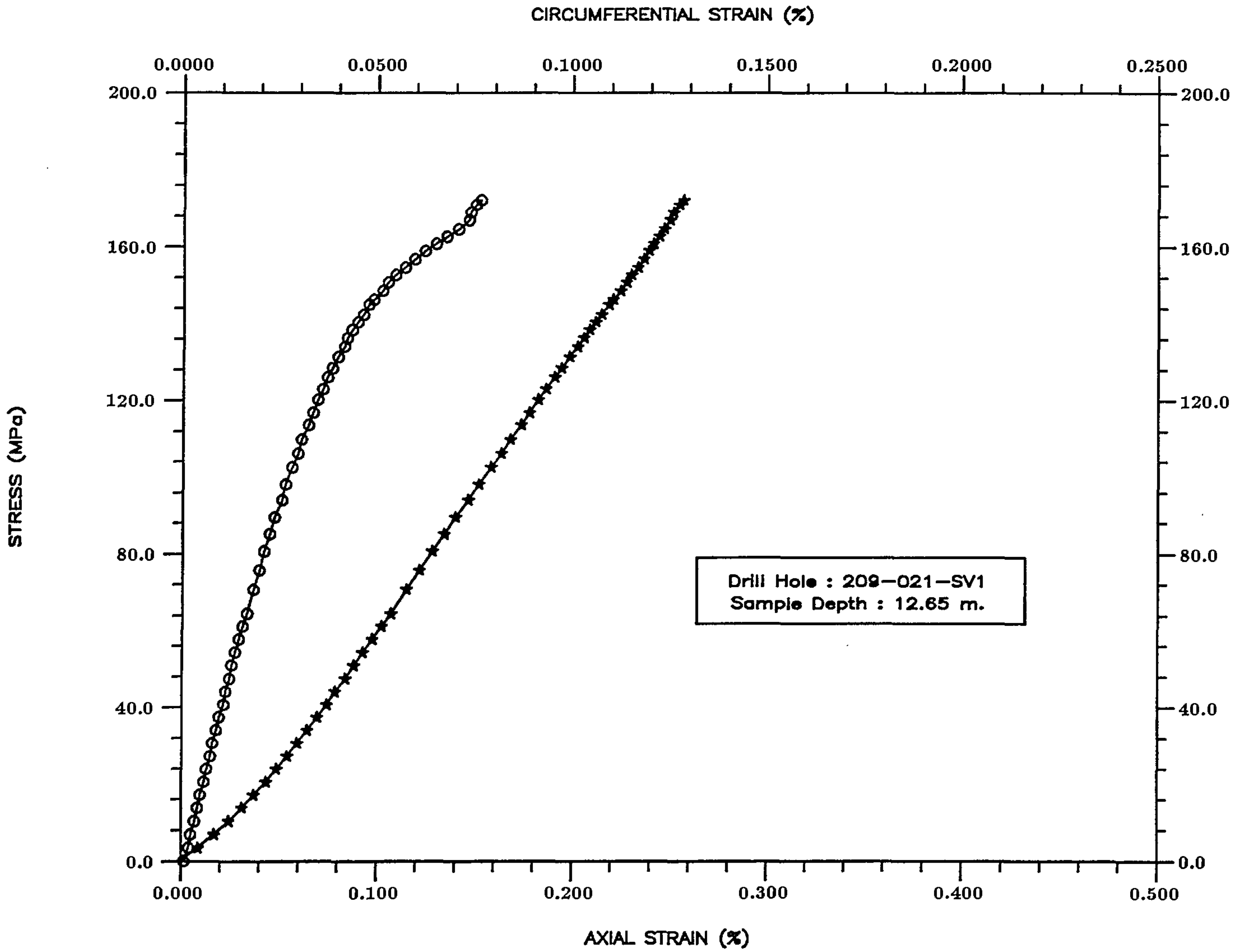

Fig. 27: Axial and circumferential stress/strain curves for anomolous uniaxial test specimens.

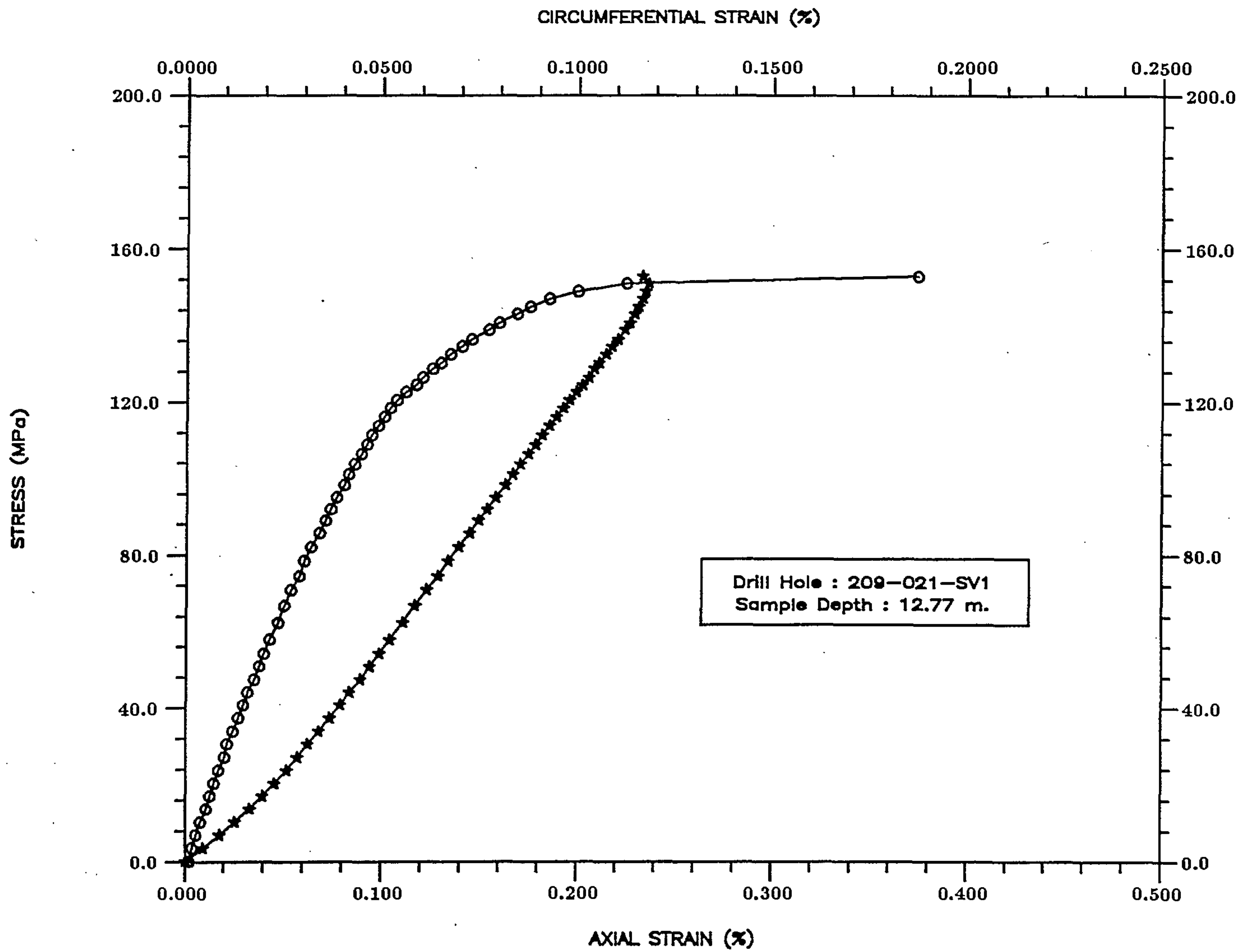

Fig. 28: Axial and circumferential stress/strain curves for anomolous uniaxial test specimens.

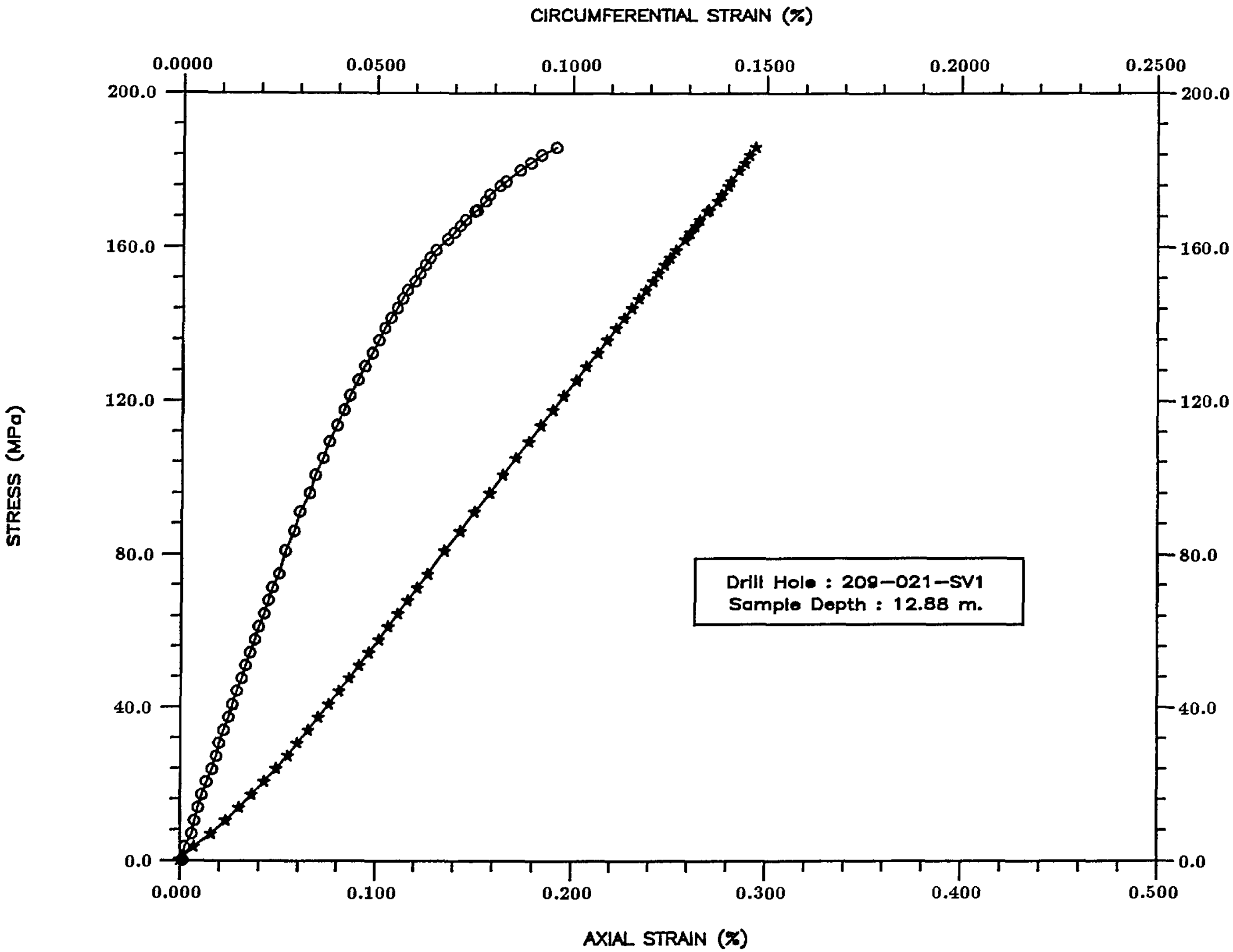

Fig. 29: Axial and circumferential stress/strain curves for anomolous uniaxial test specimens.

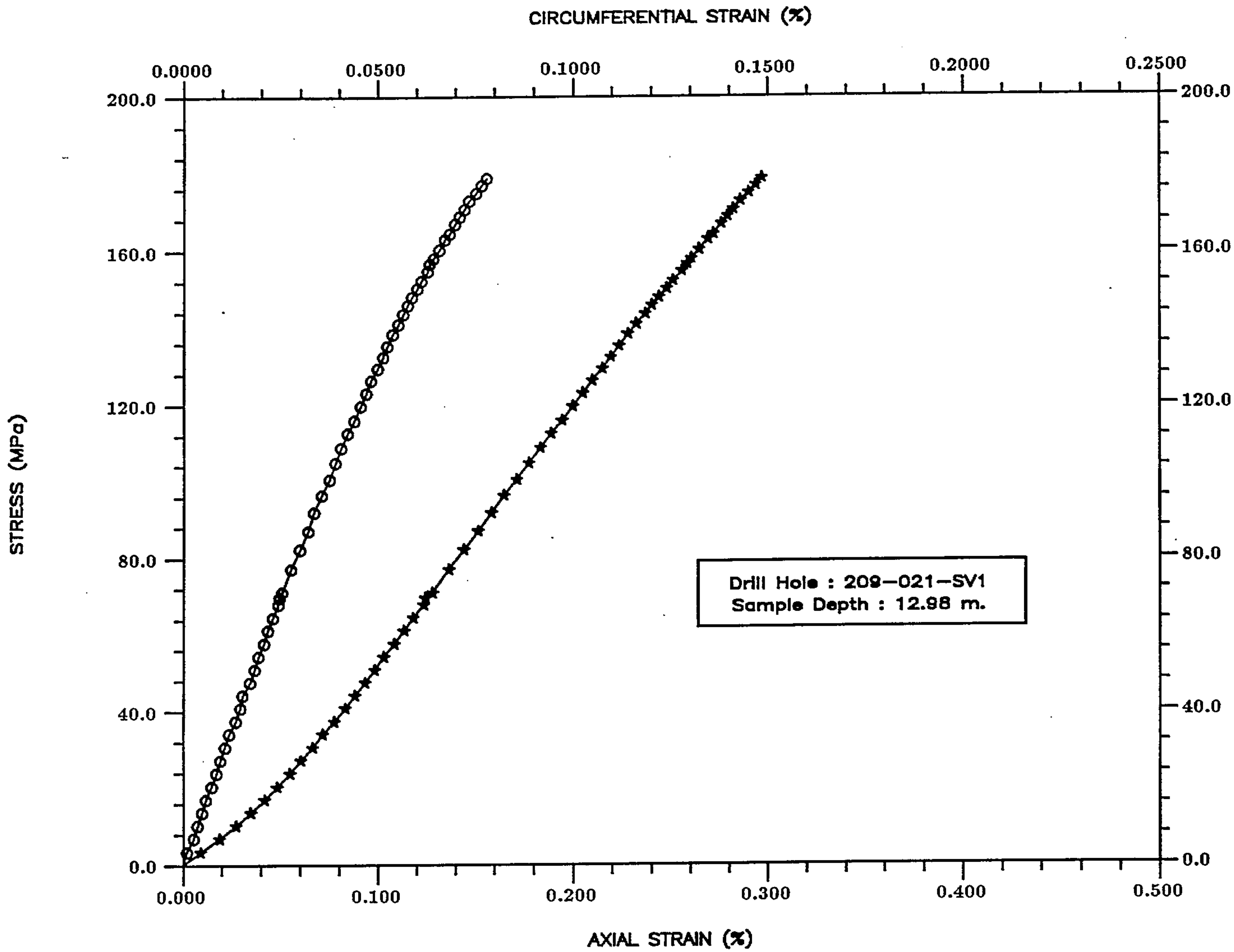

Fig. 30: Axial and circumferential stress/strain curves for anomolous uniaxial test specimens.

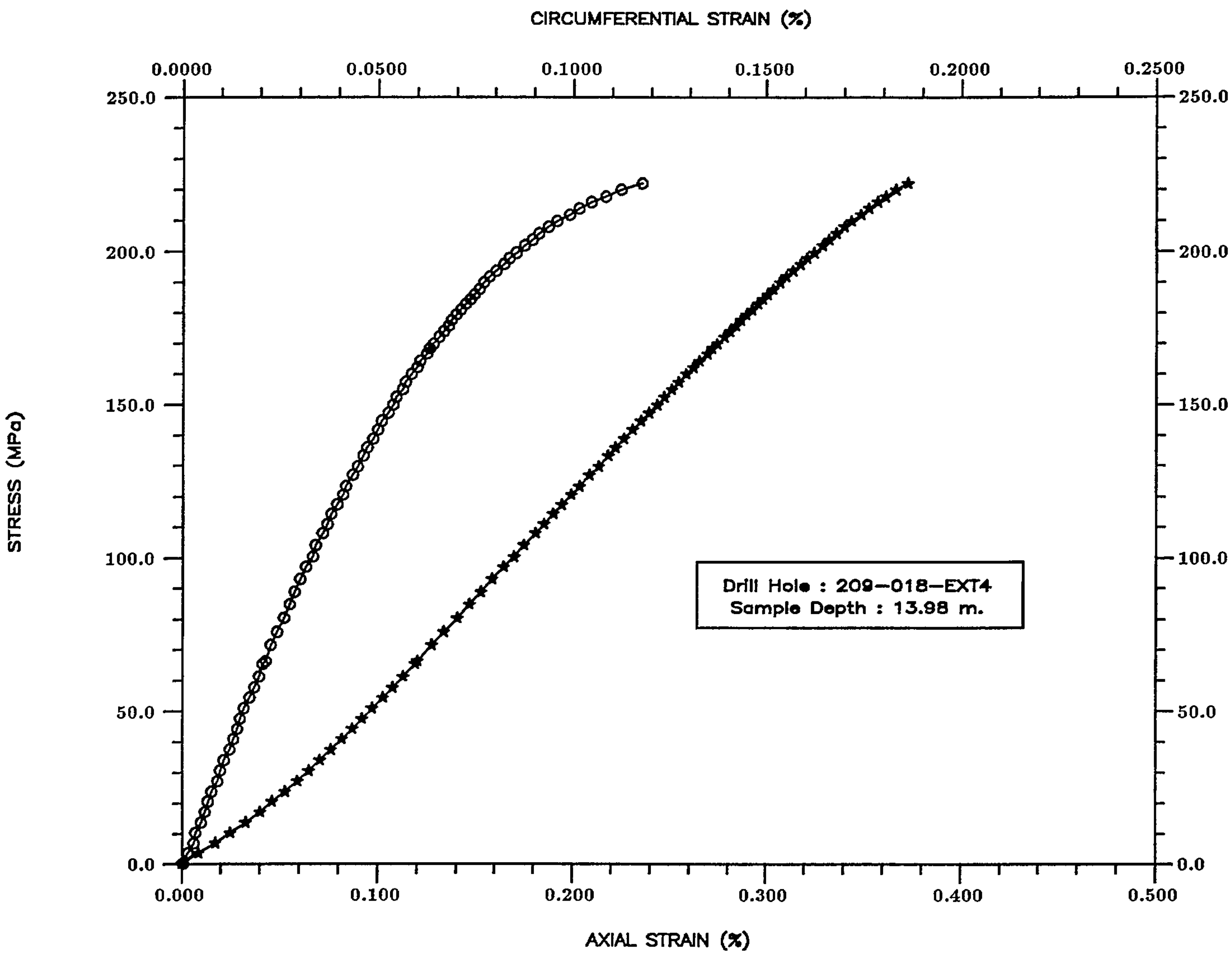

Fig. 31: Axial and circumferential stress/strain curves for anomolous uniaxial test specimens.

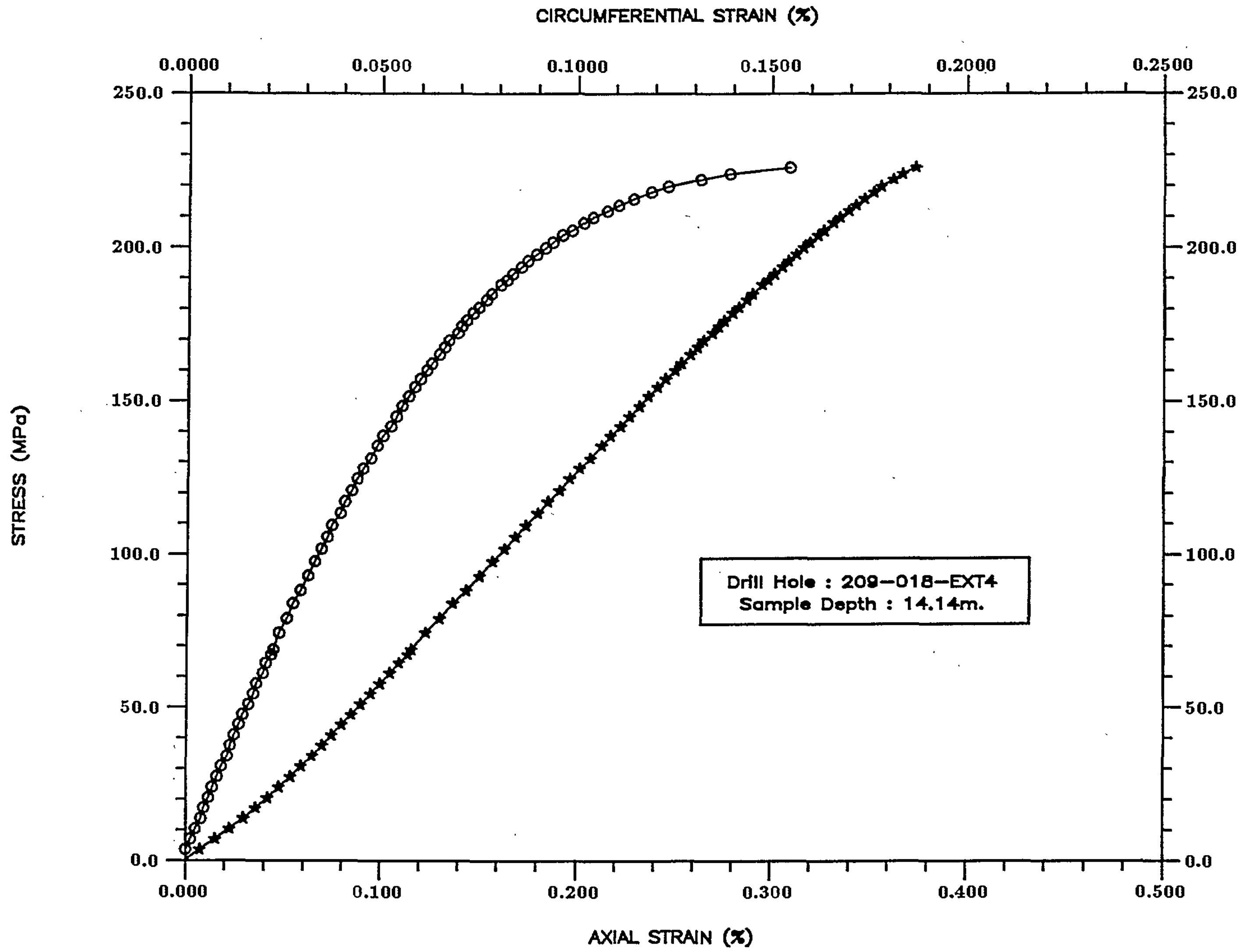

Fig. 32: Axial and circumferential stress/strain curves for anomolous uniaxial test specimens.

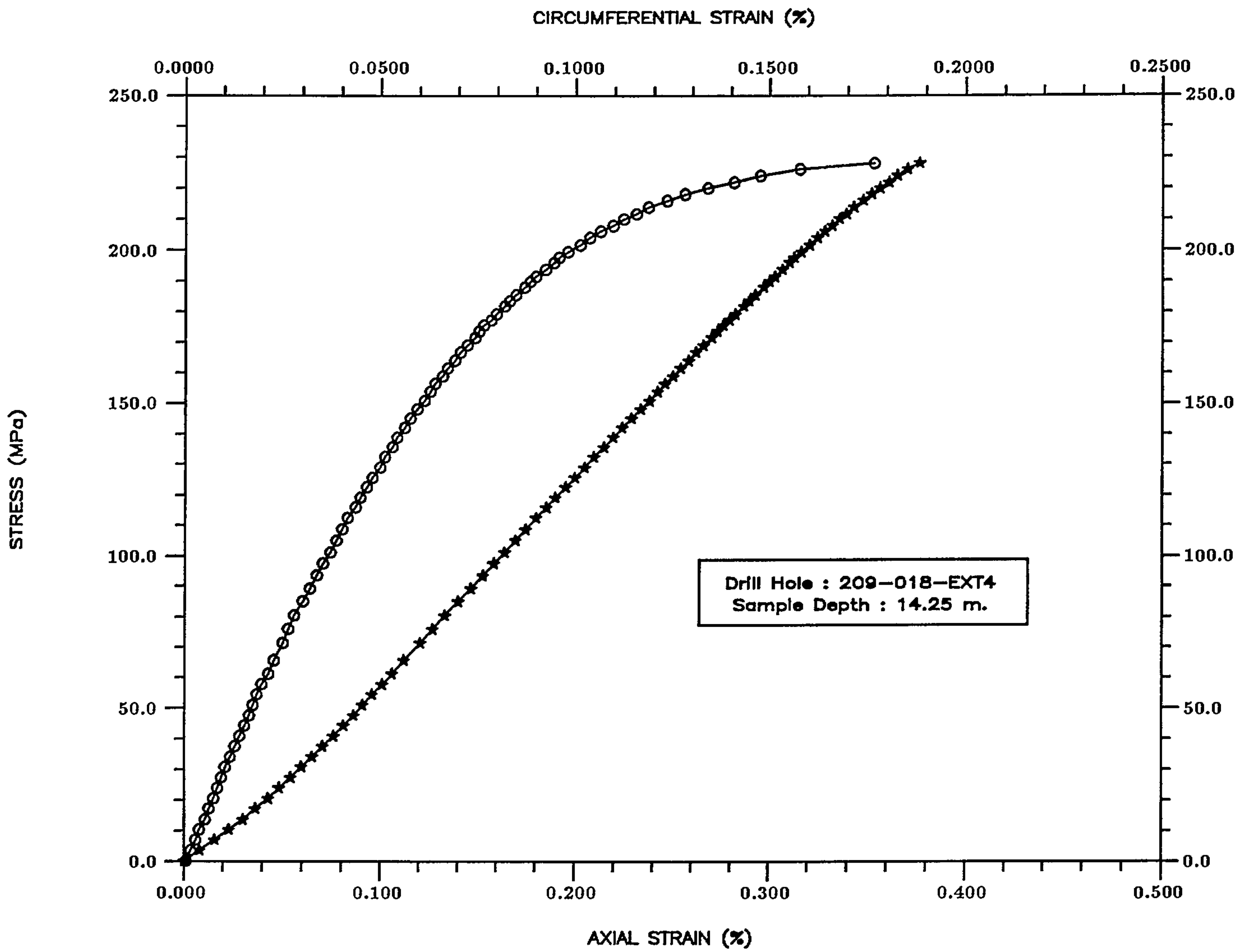

Fig. 33: Axial and circumferential stress/strain curves for anomolous uniaxial test specimens.

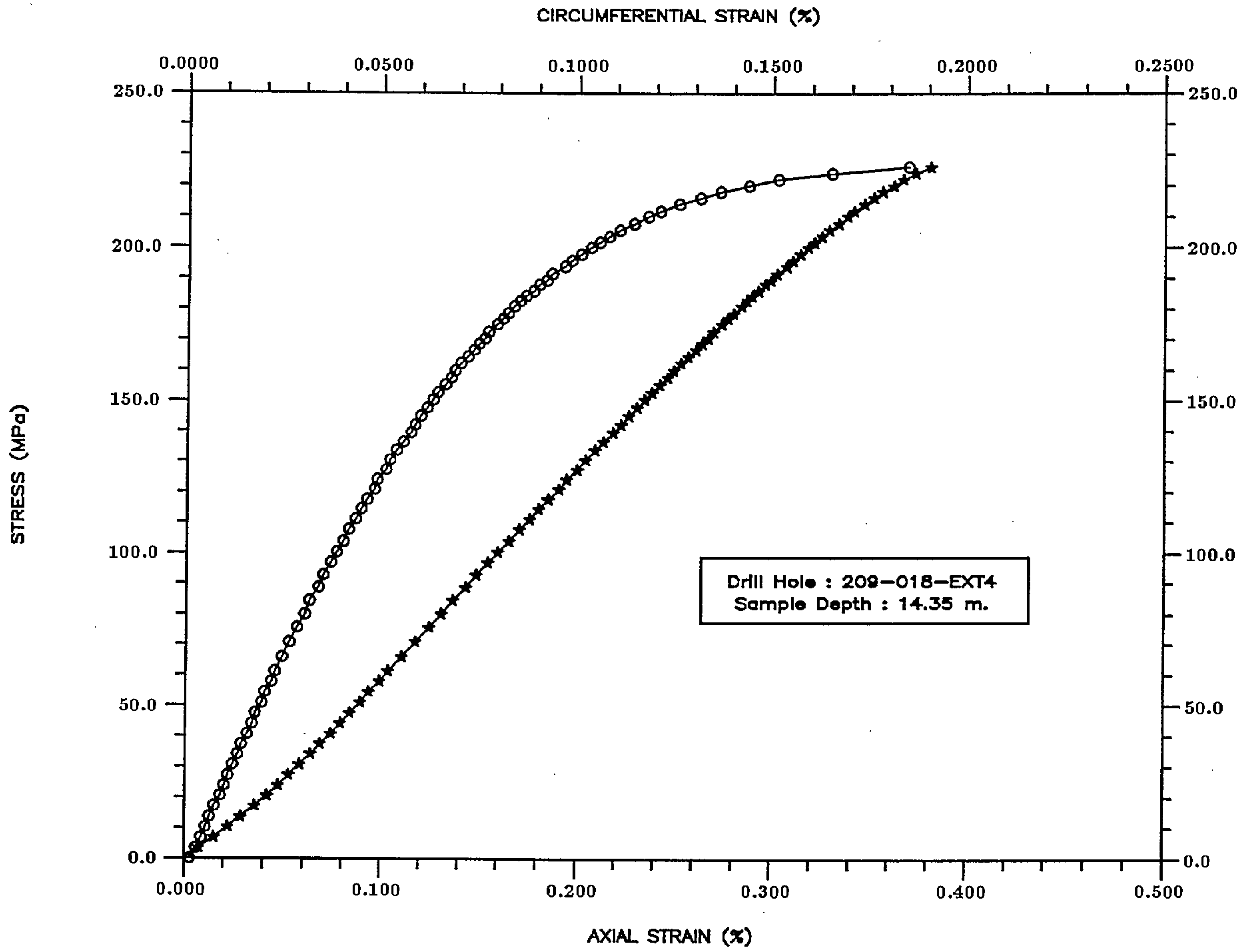

Fig. 34: Axial and circumferential stress/strain curves for anomolous uniaxial test specimens.

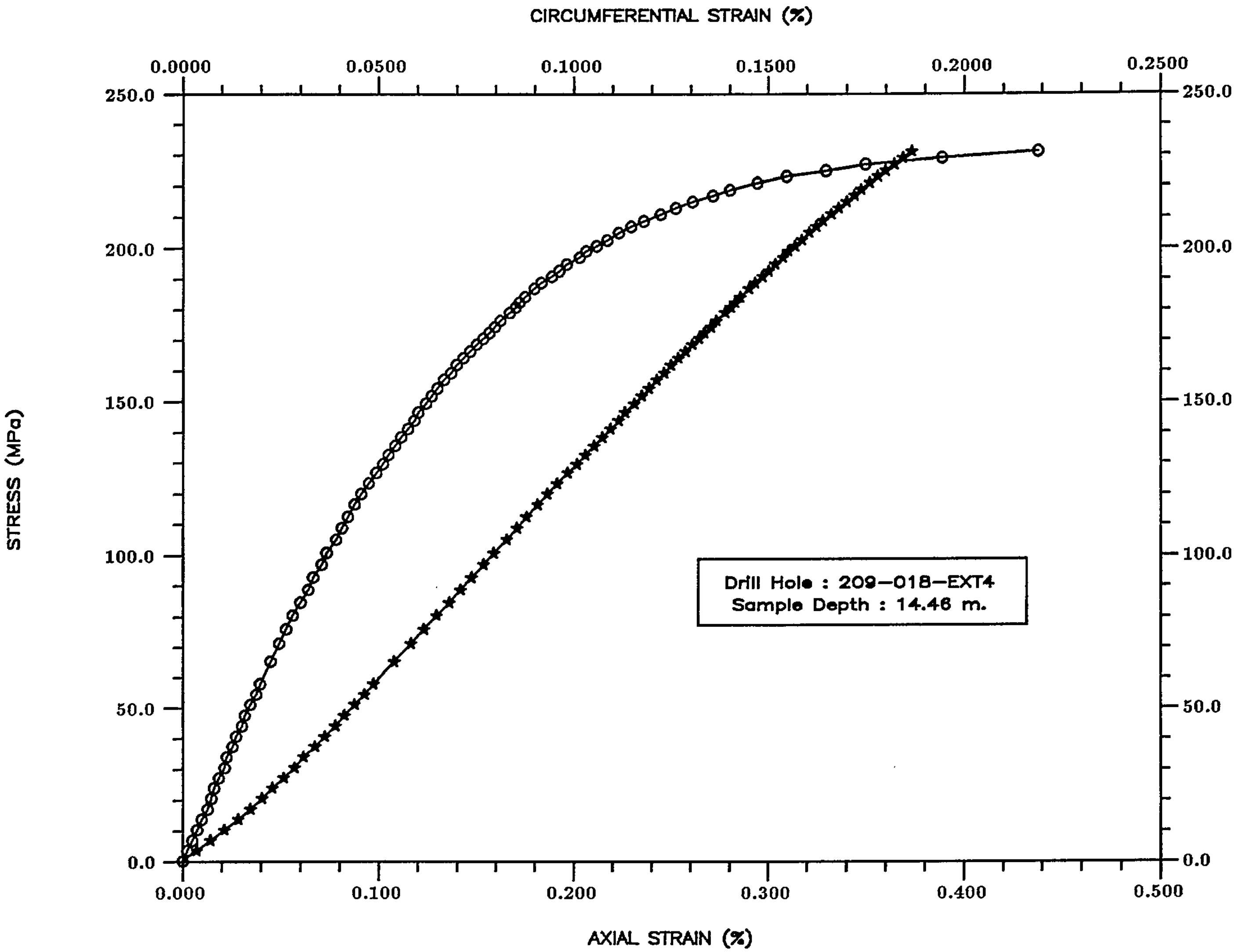

Fig. 35: Axial and circumferential stress/strain curves for anomolous uniaxial test specimens.

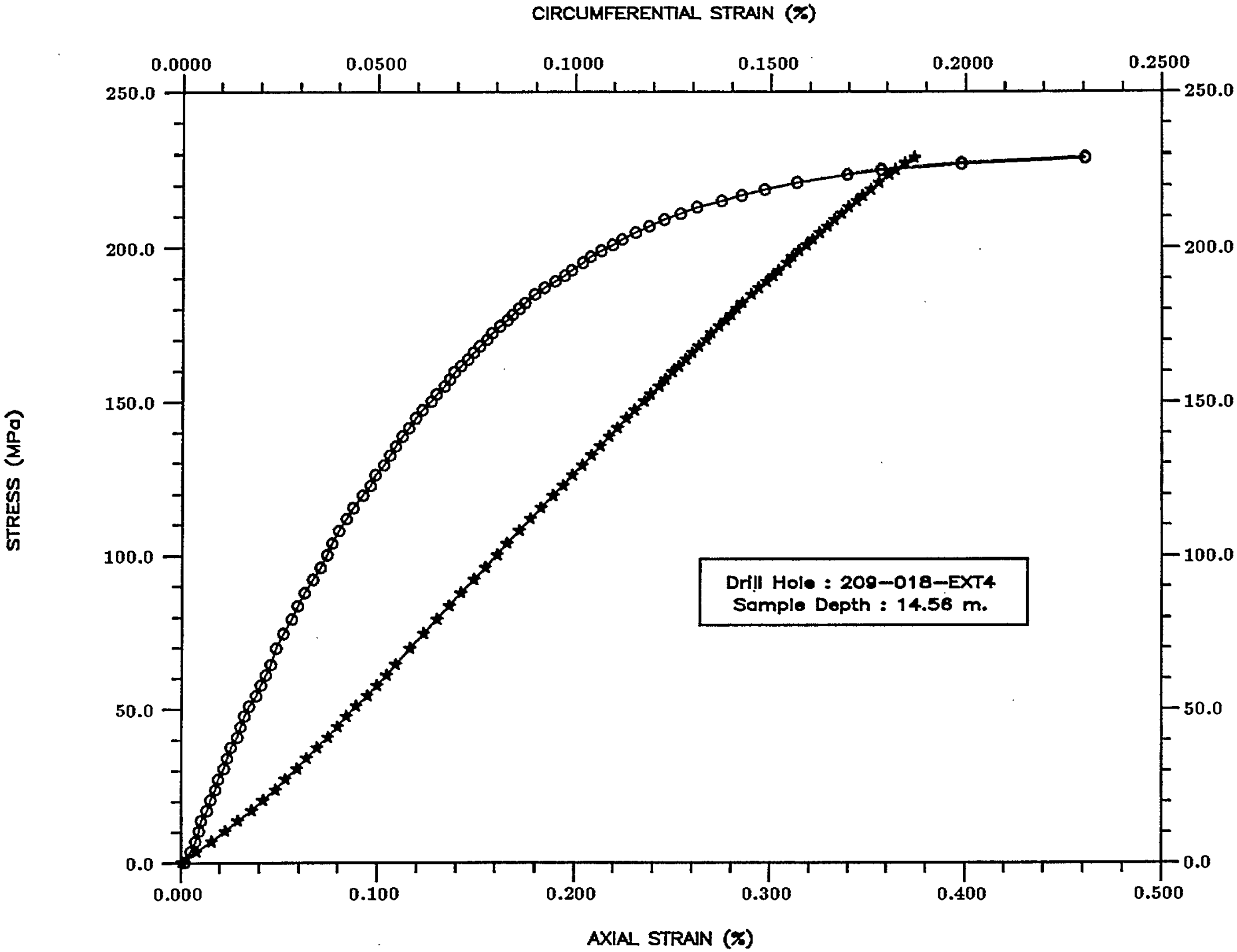

Fig. 36: Axial and circumferential stress/strain curves for anomolous uniaxial test specimens.

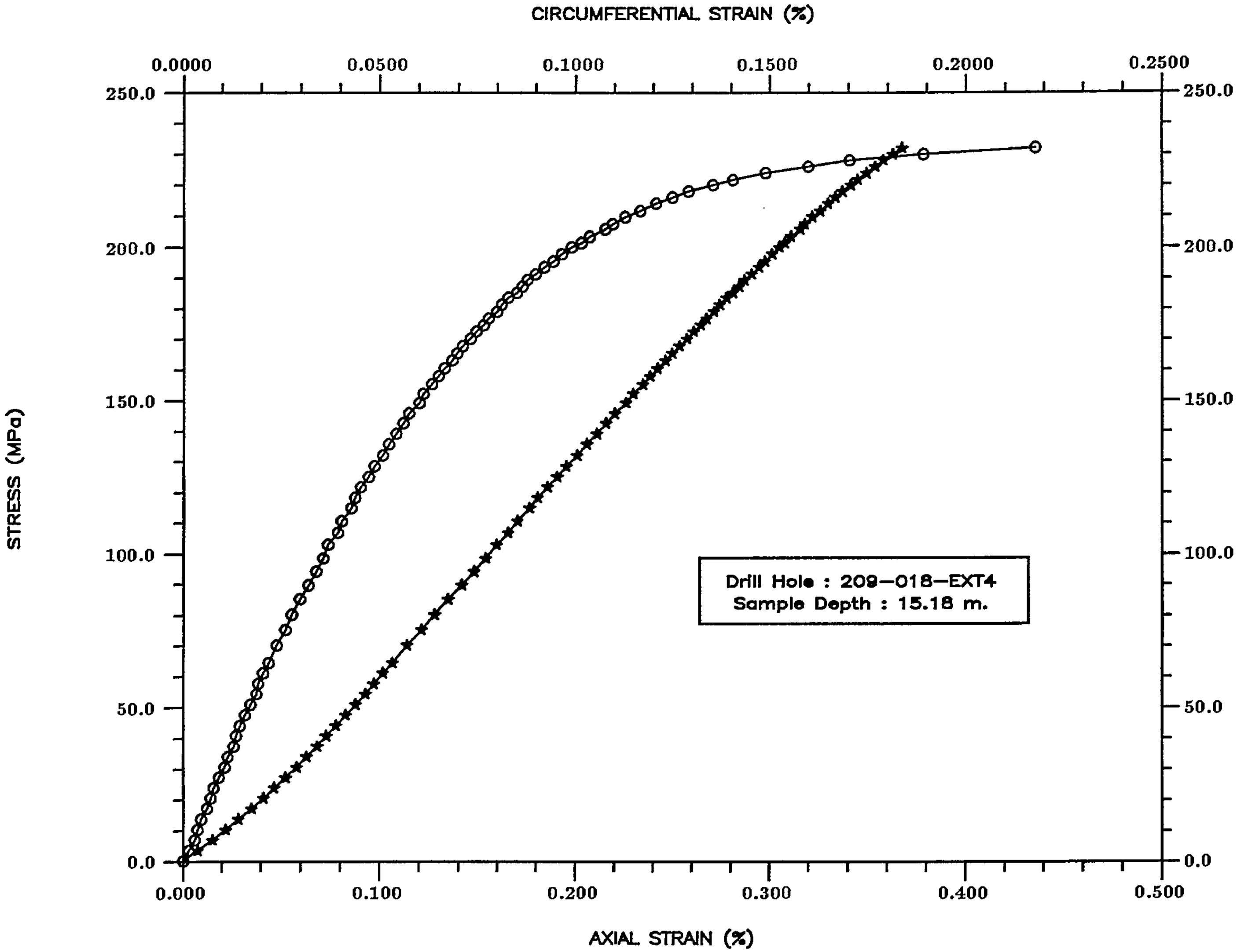

Fig. 37: Axial and circumferential stress/strain curves for anomolous uniaxial test specimens.

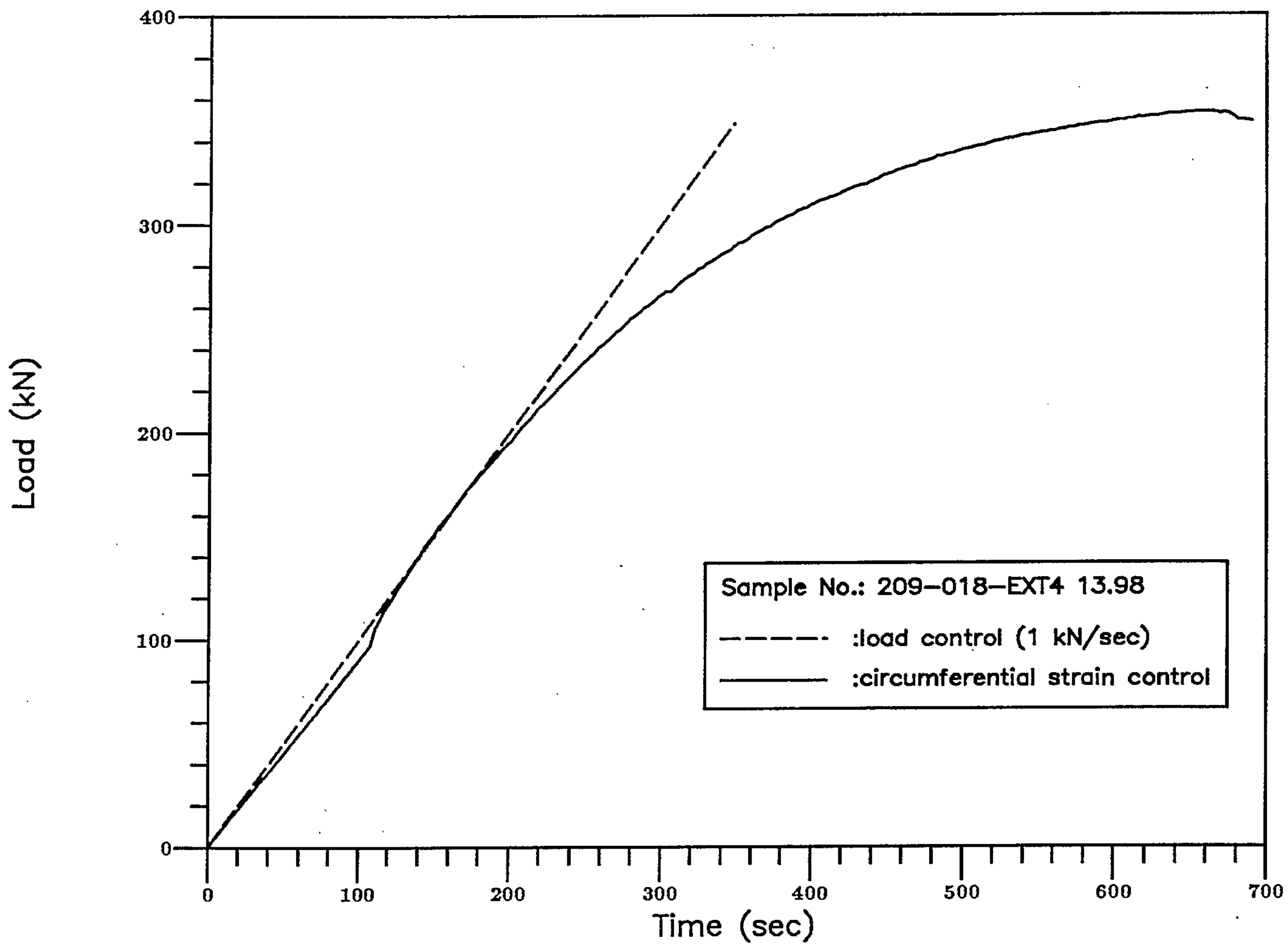

Fig. 38: Load vs time for load and circumferential strain control modes.